



Design and Thermomechanical Finite Element Analysis of Frictional Contact Mechanism on Automotive Disc Brake Assembly

Ali Belhocine · Oday Ibraheem Abdullah

Submitted: 14 December 2019 / Published online: 30 January 2020
© ASM International 2020

Abstract The braking phenomenon is an aspect of vehicle stopping performance where with kinetic energy due to speed of vehicle is transformed to thermal energy via the friction between the brake disc and its pads. The heat must then be dissipated into the surrounding structure and into airflow around the brake system. The frictional thermal field during the braking phase between the disc and the brake pads can lead to excessive temperatures. In our work, we presented numerical modeling using ANSYS software adapted in the finite element method, to follow the evolution of the global temperatures for the two types of brake discs, full and ventilated disc during braking scenario. Also, numerical simulation of the transient thermal and static structural analysis was performed here sequentially, with coupled thermo-structural method. Numerical procedure of calculation relies on important steps such that the computational fluid dynamics (CFD) and thermal analysis have been well illustrated in 3D, showing the effects of heat distribution over the brake disc. This CFD analysis helped us in the calculation of the values of the heat transfer coefficients (h) that have been exploited in 3D transient evolution of the brake disc temperatures. Two different rotor designs and three different brake disc materials were tested and comparative analysis of the results was conducted in order, to derive the one with the best thermal behavior. Finally, the resolution of the

coupled thermomechanical model allows us to visualize other important results of this research such as the deformations, and the equivalent von Mises stress of the disc, as well as the contact pressure of the brake pads. Following the analysis of the results obtained, we drew several conclusions from this investigation. The choice allowed us to deliver the rotor design excellence to ensure and guarantee the good braking performance of the vehicles.

Keywords Brake disc · Heat flux · Heat transfer coefficient · Thermomechanical coupling · Brake pad · Gray cast iron · Von Mises stress · Contact pressure

Introduction

Automobile is complex integration of electronic and mechanical components. One of the major components is the braking system which is limited due to its shortcomings.

Automotive industry faces new challenges every day, new design trends and technological deployments from research push companies to develop new models and facelifts in short term, requiring new tools or tool reshaping [1]. Conventional brakes and clutches require complex mechanical parts to transmit energy [2]. Brake rotor of an automobile is a crucial component from the safety perspective. To stop the vehicle, friction material in the form of brake pads is forced mechanically, hydraulically, pneumatically or electromagnetically against both sides of the disc [3]. During braking of an automobile, the entire kinetic energy of the moving vehicle is converted into heat energy due to friction between the brake rotor and brake

A. Belhocine (✉)
Department of Mechanical Engineering, University of Sciences and the Technology of Oran, L.P 1505 El-MNAOUER, 31000 Oran, Algeria
e-mail: belho2017@gmail.com

O. I. Abdullah
System Technologies and Mechanical Design Methodology,
Hamburg University of Technology, Hamburg, Germany

pad [4]. Pads are the major means by which mechanical forces are transferred to the surface that is being polished. However, little research has dealt with the variation of the pad characteristics due to pad wear [5]. One of the most important factors that have significant effects on the uniformity of the polished surface is the pad wear profile [6]. Non-uniformity of pad surface topography affects the contact area and friction force between the pad and wafer surface [7]. Computer-aided modeling and simulation are becoming one of the methods used frequently in research and development activities in today's automotive industry [8]. Ashraf et al. [9] presented numerical simulation of wear for a polymer–polymer sliding surface contact in dry conditions of automotive applications in which finite element analysis (FEA) used as a tool to calculate nodal pressures at the contact area for small sliding steps. Salonitis et al. [10] presented modeling and predicting of the process forces as a function of the process parameters. From this study, they investigated the effect of the grinding wheel specifications on the induced process forces of grind-hardening. Leronés et al. [11] presented an automatic total quality control system for automotive industry brake discs. A slice of the frictional heat during the braking phase of a vehicle is propagated in the atmosphere following two phenomena; in this case, radiation and thermal convection. The convection heat transfer coefficient h is not a property of the fluid. It is an experimentally determined parameter whose value depends on all the variables influencing convection such as the surface geometry, the nature of fluid motion, the properties of the fluid, and the bulk fluid velocity [12]. It is obvious, therefore, that the calculation of the heat transfer coefficient (h) in simulation and numerical modeling is very serious. However, the latter is very much to evaluate because of the complexity of the friction phenomenon in the braking phase of automobiles. Belhocine and Nouby [13] developed a finite element model of the whole disc brake assembly and validated by using experimental modal analysis. Ishak et al. [14] developed one dimensional (1D) model of leading-trailing drum-type parking brake model and then verified with experiments test bench. Choi and Lee [15, 16] combined the force equilibrium equation and the heat conduction equation to solve the problem and analyzed the transient thermoelastic instability of the disc brake. Yildiz and Duzgun [17] have studied on stress analysis of three different ventilated brake discs using the finite element method. Adamowicz and Grzes [18] developed thermal finite element analysis of a solid disc brake during single as well as repetitive braking process with different number of brake application. Duzgun [19] has studied thermo-structural behaviors of different ventilation applications on brake discs. Pevac [20] conducted numerical simulation based on computational fluid dynamics (CFD) in order to determine the wall heat

transfer coefficients and to predict the temperatures in the brake disc during braking. Hwang and Wu [21] have studied on 3D thermomechanical coupling model of temperature and thermal stress in ventilated disc brake. Han et al. [22] analyzed thermal fatigue stress of automotive brake discs by using the coupled thermomechanical finite element (FE) simulation. Han et al. [23] presented a three-dimensional finite element (FE) model of a brake system for numerical simulation in which a coupled thermomechanical analysis is carried out to confirm the non-uniform contact pressure distribution. Dufrénoy and Weichert [24] implemented a two-dimensional (2D) fully coupled thermomechanical algorithm taking into account the wear mechanism.

The main purpose of this scientific contribution is to present numerical simulation during stop braking step in order to visualize the thermomechanical behavior of the automobile brake discs while considering the generation of initial heat flow generated by friction between both parts in dry contact (the rotor and the brake pads). The novelty of the present work is to obtain numerical solutions for the thermomechanical behavior of disc brake assembly using finite element analysis software ANSYS under weak coupling. The results for various states are verified with knowing data in the literature. We focused first our intelligence on the actual evaluation of the values of convective heat transfer coefficients (HTC) as a function of time, by adopting the ANSYS CFX code of which these have been used in the prediction of the transient temperatures of brake discs while seeing the performance of three gray cast irons. So we have detailed the problem of degradation of the vehicle brake discs by thermal fatigue. Our general concern here is to identify the disc material that is more tolerant to temperature increases. Thus, the best cooling style is used in the prototype of manufacture of automotive brake discs. These results are quite in good agreement with those found in reality in the brake discs in service and those that may be encountered before in literature research investigations of which these are very useful for engineers and in the design field in the vehicle brake system industry. This simulation allowed us to visualize some important results such as, the global deformations and von Mises stress of the model (disc pads), the contact pressure distribution of the inner pads as well as, the influence of the grooved brake pad and the mode of loading exerted by the piston on the stresses established on the structure. We finally compared these numerical results with experimental results obtained from literature containing measurements of ventilated discs surface temperatures to validate the accuracy of the results from this simulation model.

The results of this analysis are in accordance with reality and the current life of the braking phenomenon and the

brake discs in service thus with the thermal gradients and the phenomena of damage observed on used discs brake.

Disc Brake System and Operation

Brake rotor is defined as any metal part generally mounted on wheels of the vehicle before the braking process, and planted to brake pads inside fixed caliper composed of piston constituting two elements: filling or friction material and sheet steel base (Fig. 1).

Brake Disc Kinds

We know in the field of the automobile, two kinds of brake discs: full discs and ventilated discs. But, there are also other types of discs such as grooved brake discs and drilled brake discs. Full discs usually have a crown attached to bowl disc which is nailed to the wheel of the vehicle (Fig. 1a).

Ventilated brake discs are modern discs of complex shape used in our time when they are equipped with front axles of vehicles by constituting two so-called broken crowns which are separated by fins (Fig. 2b). In geometric design of the ventilated brake discs, these fins provide good cooling and excellent ventilation compared to full discs by raising the area of the convective heat exchange. Indeed, the mass of the brake disc also plays an important role and it is for that, the disc rotor weight is minimized that influences the thermal input quantity that is needed to raise

the temperature of the rotor body. Taking into account the variation of elements to know; the material, the size and the geometry of the fins (circular pins, curves, radial fins), the ventilated discs are completely constructed thus guaranteeing good thermal absorption capacity.

Numerical Simulation Methodology

The heat transfer problem of the brake disc was analyzed using a coupled CFD/FEA simulation method. The CFD analysis for this study was performed in ANSYS CFX. The primary purpose of the CFD analysis was to compute the HTC's on the solid boundaries. The heat generated at the contact surfaces of the pad and disc is dissipated by the forced convection due to enlarged airflow and the natural convection after the full stop, whereas conduction absorbs energy from the interface of the friction pair. Because heat transfer coefficients (HTC's) are dependent only on temperature between the hot body and the fluid, during the natural convention, when the forced convention takes place, the HTC depends also on the fluid velocity around the hot body, it was necessary to couple the CFD and FEA solutions. These produced HTC versus time curves. An iterative process of transferring HTC's from CFD to FEA was developed. The temperature distribution of the disc brake rotor was calculated using the FEA model. In our case, where the thermal and mechanical problems are decoupled, it is advisable to resort to a weak coupling resolution consisting of first determining the temperature

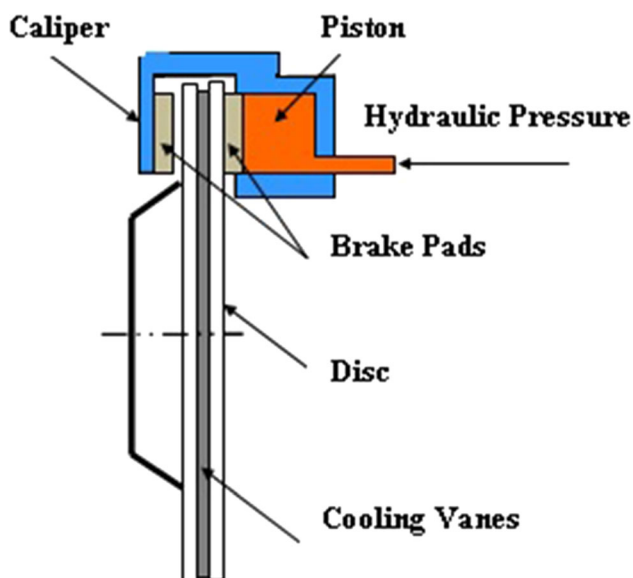


Fig. 1 The composition of braking system

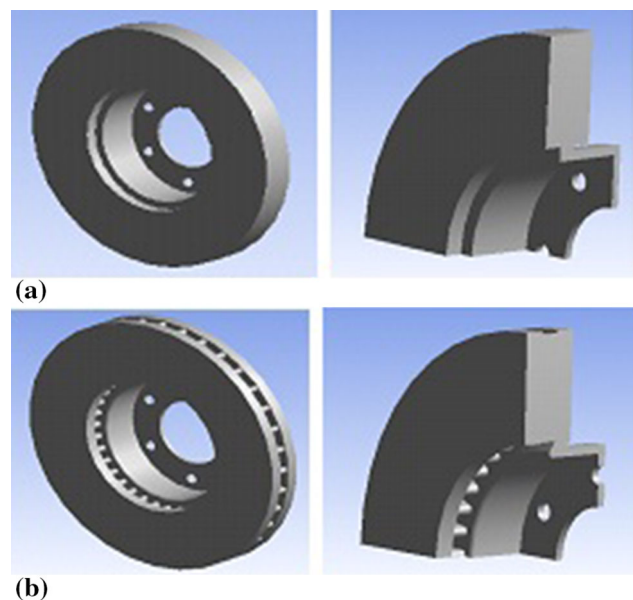


Fig. 2 CAD model of discs brakes: (a) full disc (b) ventilated disc

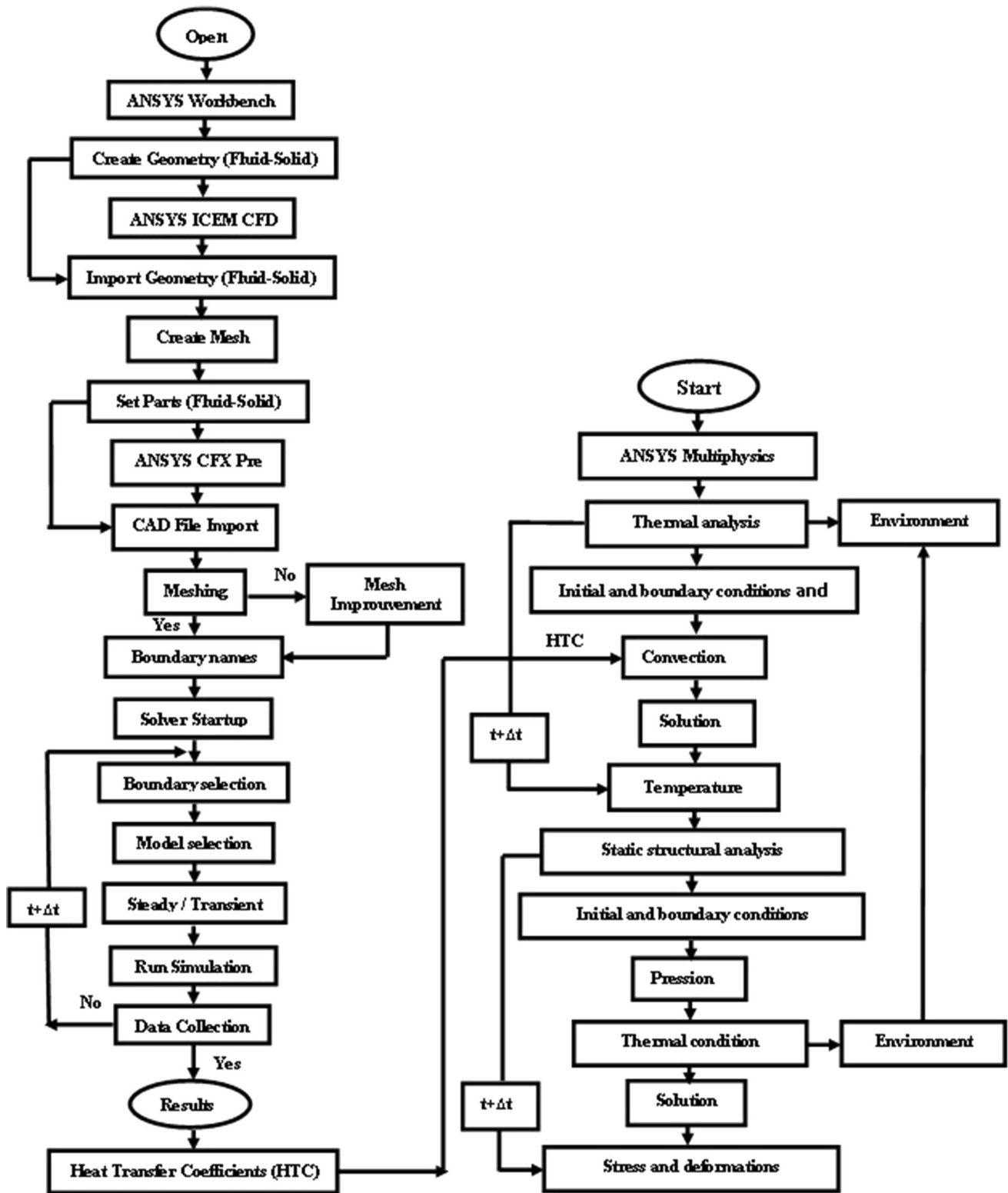


Fig. 3 Flowchart of present methodology

field independently of the mechanical conditions and then evaluating the stresses and deformations induced by this temperature field. The step by step process of solving a coupled thermomechanical problem is highlighted as a flowchart in Fig. 3.

CFD Modelling and Analysis with ANSYS CFX

Any solution of nonlinear partial differential equations describing turbulence problems, fluid motion and heat transfer phenomena as well as; the vehicles aerodynamics problem is essentially based on the procedure of the CFD. With precise solution of these equations using this adopted procedure, fast and reliable convergence can be achieved while estimating the physical parameters of the fluid flow as speed, temperature, viscosity, and pressure.

Solution Procedure of CFD Analysis

ANSYS CFX software is high-performance advanced resolution technology used especially in the field of CFD, as large flow solution application, it allows us to provide highly accurate, reliable, robust and fast solution results. ANSYS CFX consists of three modules that communicate with each other as shown in Fig. 4. Software that allows the realization of geometry and mesh is required to perform a CFD analysis.

Governing Equations

In this analysis, we presented a simplified model and simulation of surface heat flux in the brake disc caused by friction while using ANSYS CFX software. The model that was discussed here in this study is similar to that developed by Palmer et al. [25]. All equations used in CFD analysis, namely the Navier–Stokes moment equation, the energy equation, and the continuity equation, were used to solve

the thermal problem, which is the variation of heat transfer and air flow around the brake disc.

(a) Continuity equation:

The mass conservation equation in the case of compressible and incompressible flows is defined as follows

$$\frac{\partial \rho}{\partial t} + \nabla \cdot (\rho u) = S_m \tag{Eq 1}$$

where, S_m is the mass added to the continuous phase from the dispersed second phase.

(b) Momentum (Navier–Stokes) equations:

In inertial frame, the governing momentum conservation equation is given by the form:

$$\frac{\partial(\rho v)}{\partial t} + \nabla \cdot (v v) = -\nabla p + \nabla \cdot (\tau) + \rho g + F \tag{Eq 2}$$

where the stress tensor τ is of the form:

$$\tau = \pm \mu \left[(\nabla v + \nabla v^T) - \frac{2}{3} \nabla \cdot v I \right] \tag{Eq 3}$$

The left term of Eq 2 can be reduced to the form below by using the rotating reference frame (RRF) technique in the case of rotating brake disc and in absolute velocity.

$$\frac{\partial(\rho v)}{\partial t} + \nabla \cdot (\rho v_r v) + \rho(\Omega \times v) \tag{Eq 4}$$

where, Ω and v_r are, respectively, the angular velocity and the absolute velocity, the continuity equation used in analysis (RRF) is expressed;

$$\frac{\partial \rho}{\partial t} + \nabla \cdot (\rho v_r) = S_m \tag{Eq 5}$$

Heat Flux Entering the Disc

During active braking process of moving vehicle, its kinetic energy is converted to heat energy by dry friction between the two parts (disc and brake pads) producing a distribution of heat flux on both sides of the disc. The general formula for calculating the initial flux entering the automotive brake disc can be expressed as follows [26]. This formulation is detailed in “Appendix 1.”

$$q_0 = \frac{1 - \phi}{2} \frac{m g v_0 z}{2 A_d \epsilon_p} \tag{Eq 6}$$

where g is the acceleration of gravity (9.81) (m/s²), a is the vehicle deceleration (m/s²), $z = a/g$ is the braking efficiency.

The quantity evaluated using Eq 6 of the initial heat flux has been exploited of course in first step of the CFD analysis and then in transient thermal analysis using finite element software ANSY Workbench 11.0 to visualize the variation of the brake disc temperature.

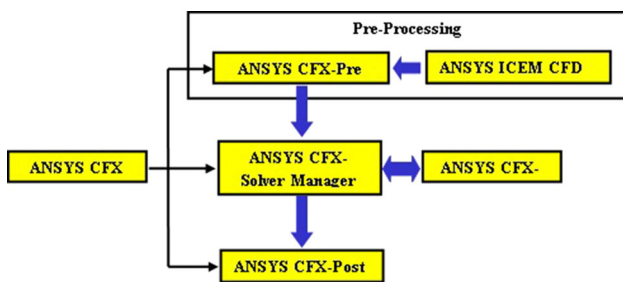


Fig. 4 ANSYS CFX code structure

In this contribution, we evaluated the transient values of the heat transfer coefficient (HTC) by using ANSYS CFX software, which has been substituted in multiphysics analysis to predict the three-dimensional temperature (3D) of the brake disc. In fact, this latter absorbs an amount of more than 90% of the thermal energy generated by friction [27]. Given the complexity of the phenomenon treated, we assumed that the thermal flux entering the rotor, and the

brake pads replace the effect of dry friction between the two bodies in contact, as shown in Fig. 5.

The heat flux generated in the rotor area is considered a thermal loading. In our scientific contribution, we used ventilated brake disc made of high-carbon gray cast iron material FG, whose disc having the geometric dimensions (262×29 mm) equipping certain types of vehicles (Fig. 6).

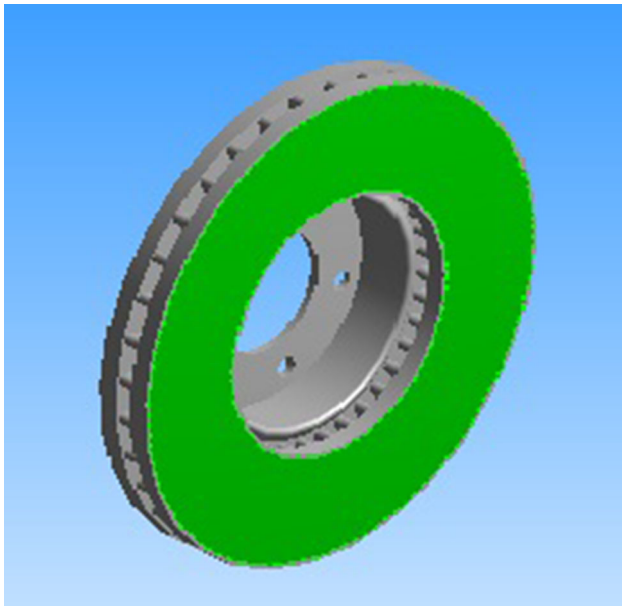


Fig. 5 Heat flux from braking friction

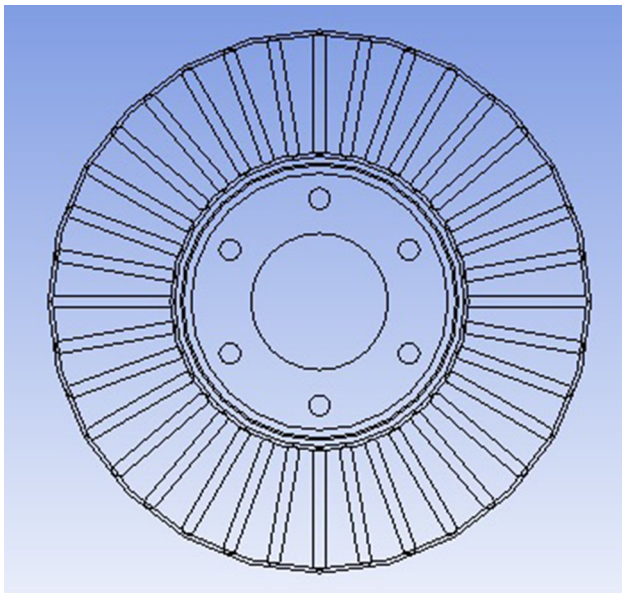


Fig. 6 Contour view of ventilated disc

k - ϵ Turbulent Model

The turbulence model (k - ϵ) is the most widely used model in the field of CFD analysis as numerical simulation of the average flow characteristics in the turbulent flow regime. It is a two-equation model that gives general description of turbulence using two partial differential equations (PDE) called the transport equation, one for turbulent kinetic energy (k) and other for dissipation (ϵ). For current models, the model provides a good agreement for accuracy and virility.

Modelling Assumptions

Many studies of brake disc channels are performed in isolation without the influence of the wheel rim and the external airflow. The choice of model complexity and simplifications are important in order to obtain a working and manageable simulation while still capturing the relevant physics of the task. To simulate the cooling dynamically with changing vehicle speed and temperatures, etc. would be too complex and computationally expensive. Due to this it was decided to conduct the simulations at a fixed speed.

The wheel and the wheelhouse are particularly important as they have strong influence on the flow behavior around the brakes. A reasonable calculation time was however needed, in order to be able to simulate numerous different concepts.

Generally, the calculation time increases with increased size of the computational domain, because of the number of cells needed. Therefore, it was not possible to use the full vehicle body in the simulations. It was decided to utilize a relatively small computational domain with a geometrical model consisting of a partial car body with rotor outside wheel rim and facing cold air.

In order to facilitate CFD calculations, we have introduced the assumptions that are summarized as:

- The flow medium is air.
- The vehicle starts with initial speed of 28 m/s.
- The pure nature of the fluid in calculation is air.
- The inlet air speed is fixed at 28 m/s.

- The regime is steady-state turbulent incompressible flow around the disc brake rotor according to the turbulence model $k-\epsilon$.
- The thermophysical properties taken into account in the calculation are constant like (viscosity, specific heat, thermal conductivity, and density).
- The radiation phenomenon is neglected, whereas only conduction and thermal convection are considered here.
- The distribution of heat flux on area of the brake disc is quite uniform.
- Under normal pressure and temperature conditions, the physical properties of the air are considered.
- Heat Flux is uniform over pad area.
- Brake disc absorbs almost 90% of thermal friction.

CFD Analysis with ANSYS CFX

In studies, much attention was paid to characteristics and complex nature of the flow around the rotating disc (s), whether it be laminar, regular swirling, axisymmetric, or thermal transfer [28, 29]. Knowledge of the coefficient of exchange (h) in the flows is important and in the large backwater simulation, the renormalization group (RNG) $k-\epsilon$ turbulence model is usually considered desirable choice regarding rotation or swirling flow.

Various external and internal faces of the two structures, full and ventilated disc that were derived from the code ANSYS ICEM CFD are shown in Figs. 7 and 8.

Finite volume method is common approach used in the ANSYS CFX codes is essentially based on the elements to which the discretization according to mesh of the spatial domain gives us finite volumes that are exploited for the conservation of the high quantities, namely the energy, mass, and momentum. Mesh normally in CFX is in three

dimensions, nevertheless in order to simplify things; this one has been demonstrated only in double dimensions.

The mesh is realized here, in linear tetrahedral elements with 179,798 elements and 30,717 nodes (Fig. 9). ANSYS CFX code solves the CFD aerodynamic model of the brake disc while basing on transitory type of the problem whose all boundary conditions were injected in both domains (solid and fluid).

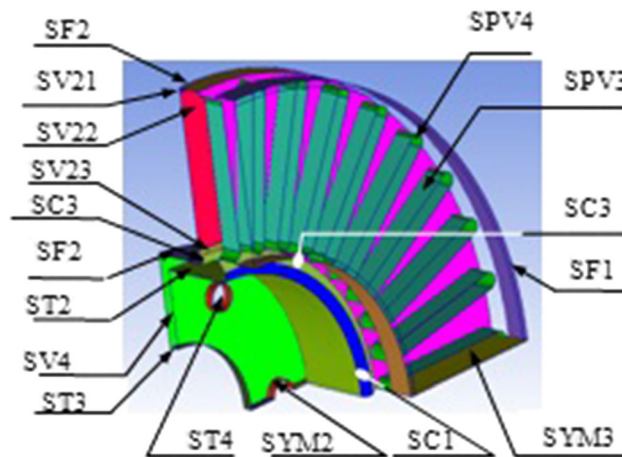


Fig. 8 Quarter of the ventilated disc showing the assignment of face names

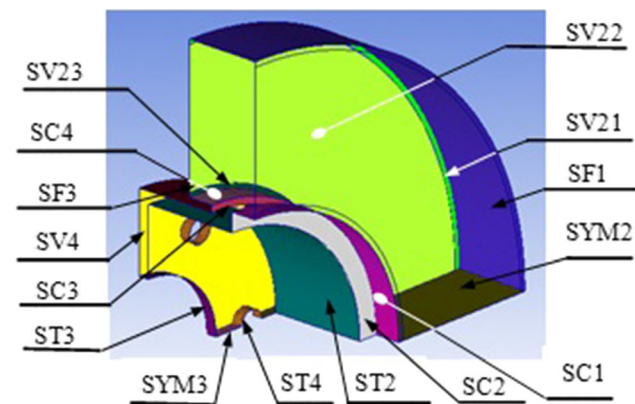


Fig. 7 Quarter of full disc showing the assignment of face names in the simulation

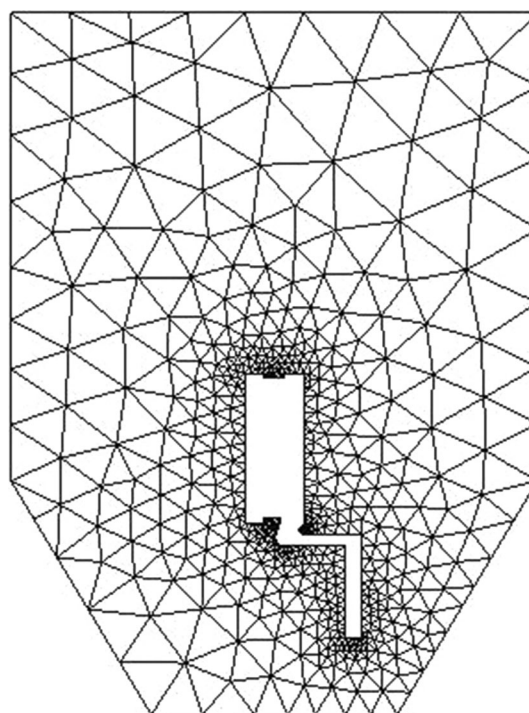


Fig. 9 Wall meshes for the CFD simulation

In this study, we have considered that the ambient air temperature at 20 °C surrounding the brake disc is equal to it in the initial state, zero relative pressure of which has been maintained at the high, low and radial edges of the fluid domain.

Fluid Mesh Generation

In this study, the mesh generated on the model characterizing the fluid domain is tetrahedral mesh containing 179,798 elements, and 30,717 nodes. Actually, ventilated brake disc consists of two full discs connected to each other internally by fins that form tunnels with open side for the passage of air to flow from the inside diameter and out to the outer diameter of the disc. Centrifugal force due to disc rotation forces the air in the channels to flow outwards to the perimeter of the disc. This creates a continuous flow of air from the access zone and exits from outside to ambient air in the area called air outlet area. Due to symmetrical shape of the brake disc, we modeled only quarter of the fluid domain geometry using ANSYS ICEM CFD software (The Integrated Computer Engineering and Manufacturing code for Computational Fluid Dynamics (ICEM/CFD)) which gives us the graphical interface shown in Fig. 10.

Boundary Conditions and Computational Details

Any simulation on ANSYS software for its version ANSYS Mechanical or Multiphysics makes it possible to define database or materials properties that characterize the elements to be analyzed. These are integrated directly from ANSYS Workbench into the materials library taken at air temperature at 20 °C before any preliminary step. In the present study, we have selected three types of gray cast iron materials used in the design of brake discs to study their

performance, in this case, gray cast irons (FG25AL, FG20, FG15). Disc brakes must withstand very strong mechanical and thermal stresses in performing its stopping duty.

High carbon fires are also the most commonly used materials in the automotive industry because of their advantageous thermal and tribomechanical properties. The strength and hardness of ferrite are greater in cast iron than in steel due to the hardening effect of silicon. Cast irons have compressive strength 3–4 times higher than their tensile strength. We introduced the temporal conditions of the simulation of the braking process in ANSYS Workbench platform taking 3.5 s as the braking time to time step increments of 0.01 s. In this calculation, given the symmetry of the disc and the periodic repetition due to rotation of the rotor, the entire model of the disc is reduced and simplified to only a quarter to reduce the calculation time for simulation, that is why the conditions boundary, periodic and symmetrical have been so designated.

In order to easily model the rotational aspect of the automobile brake disc in the environment, the output and inlet edges of the fluid model are maintained in atmospheric temperature and pressure. The surrounding air temperature of the disc is set at 20 °C using rotating reference frame for the management of the moving brake disc. Symmetrical boundary conditions are also used to produce shear walls with zero shears. CFD model developed in ANSYS CFX used in search for exchange coefficient values (*h*) is well shown in Fig. 11.

Finite-Element Modelling

Finite element method (FEM) consists of approaching, in a finite-dimensional subspace, problem written in variation form (as minimization of energy, in general) in an infinite

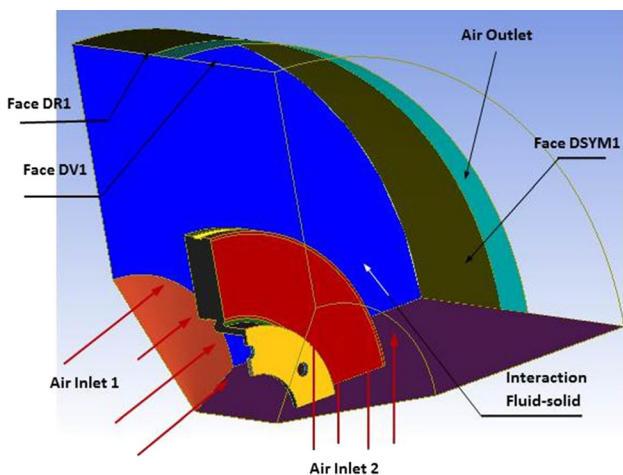


Fig. 10 Fluid body surfaces in ANSYS ICEM CFD

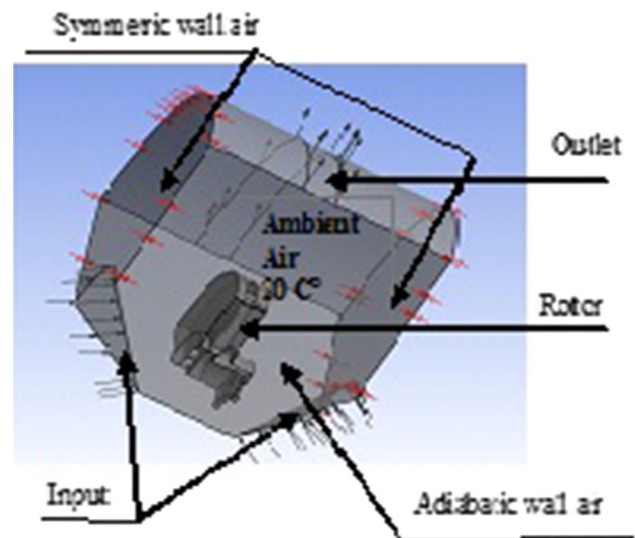


Fig. 11 CFD model of ventilated disc brake

Table 1 Design parameters of brake disc

Parameter	Value
Inside diameter of the disc (mm)	66
Outside diameter of the disc (mm)	262
Disc thickness (TH) (mm)	29
Disc height (H) (mm)	51
Weight of the car m (kg)	1385
Initial velocity v_0 (m/s)	28
Deceleration a (m/s ²)	8
Time of braking t_b (s)	3.5
Effective disc radius R_{disc} (mm)	100.5
Ratio braking forces distribution ϕ (%)	20
Factor of disc charge distribution (ϵ_p)	0.5
Disc's swept area A_d (mm ²)	35,993

Table 2 Properties of the disc and pad

Material properties	Disc	Pad
Thermal conductivity, k (W/m °C)	57	5
Volumetric mass density, ρ (kg/m ³)	7250	1400
Specific heat capacity, c (J/kg °C)	460	1000
Poisson's ratio	0.28	0.25
Friction coefficient, μ	0.2	0.2
Young modulus, E (GPa)	138	1

dimensional space. The approximate solution in this case is a function determined by finite number of parameters such as, its values at certain point (the mesh nodes). Its advantages lie mainly in possible treatment of complex geometry, more natural determination of boundary conditions, the possibility of mathematical convergence demonstrations and error enhancement. On the other hand, its disadvantages sum up in the complexity of the implementation and cost of computing time and in memory.

Modelling Assumptions

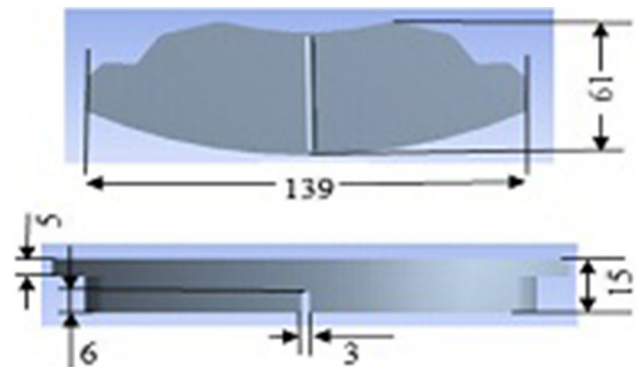
The standard dimensions of the full and ventilated brake disc are identical in this numerical simulation to ensure a better comparison of the results. Table 1 lists all the physical parameters and the geometric dimensions of the brake disc used in numerical calculations.

The disc is made of gray cast iron FG 15 with high carbon content [30], having excellent tribological and thermomechanical properties and the brake pad in semi-metallic steel fibers shows isotropic elastic behavior [31].

The brake pads were designed based on the material data of standard friction material. Semi-metallic pads are

Table 3 Design parameters of the disc and pads

Design characteristics	Disc	Pad
Volume (m ³)	9.5689e−004	8.5534e−005
Surface (m ²)	0.24237	1.8128 e−002
Mass (kg)	6.9375	0.44975
Inertia moment Ip1 (kg m ²)	3.5776e−002	2.7242e−005
Inertia moment Ip2 (kg m ²)	6.9597e−002	1.5131e−004
Inertia moment Ip3 (kg m ²)	3.5774e−002	1.2863e−004

**Fig. 12** Geometric characteristics of brake pads

strong, conduct more heat away from the rotors due to more metallic content, generate more noise and are rougher to increase rotor wear. They have low to medium coefficient of friction ranging from 0.20 to 0.38. The coefficient of friction depends upon the applied pressure, velocity, temperature, surface conditions of the pad and disc, and material properties [32] but in FEA analysis and at all times, it is assumed to be constant at to represent an average behavior. The material properties of the model are shown in Table 2, and the model was run under a constant frictional coefficient of 0.2 [31]. Design characteristics of the parts are also provided in Table 3.

Figure 12 shows the geometrical model of the brake pad used in the simulation having a height of 139 mm, a width of 61 mm, a thickness of 15 mm, and a depth and width of groove of 6 and 3 mm, respectively.

Research investigations showed the difficulty of to actually model rotating brake disc, due to simultaneous interaction of several tribological and vibro-thermomechanical phenomena during automotive braking. Nevertheless, these tips can be solved numerically and in approximate way on the basis of certain reducing hypotheses, allowing solving these problems quickly. Series of reasoning hypotheses have been applied here, throughout the duration of the braking [33]. The assumptions made while modeling the process are given below:

- In this simulation, two modes of heat transfer by conduction and convection are considerable in internal and external faces of the brake disc in such way that the radiation exchanges are negligible [34].
- The kinetic energy of the vehicle which is dissipated during the braking mechanism is totally converted into heat energy represented by a heat flux distributed on the faces of the brake disc.
- The kinetic energy of the vehicle is lost through the brake discs, i.e., no heat loss between the tire and the road surface and deceleration is uniform.
- The initial temperature of the disc is constant and is equal to the air temperature of the environment at 20 °C.
- The physical properties of the brake disc material are isotropic and homogeneous and their thermal properties are dependent on temperature.
- During the braking time, the inertia and all other forces are considered negligible.
- The domain is considered as axis-symmetric.
- Brake distribution is 60% on front, 40% on rear.
- Force distributed on one brake disc is equal to the total frictional force applied on rubbing surface.
- Before the braking phase, the brake disc is free of any stress.
- All parts of the brake disc are subject to the phenomenon of thermal convection such as the outer ring diameter area, the outer ring diameter area, the cooling fins, and the disc brake surface.

Conductivity as well as specific heat capacity of the brake disc material [35] are varied with temperature as shown in Figs. 13 and 14.

Auxiliary Equations

The general three-dimensional heat transfer equation in isotropic material in Ω domain is given as follows

$$-\left(\frac{\partial q_x}{\partial x} + \frac{\partial q_y}{\partial y} + \frac{\partial q_z}{\partial z}\right) + Q = \rho c \frac{\partial T}{\partial t} dx dy dz \quad (\text{Eq 7})$$

where $T(x, y, z, t)$ is the temperature field, ρ is the density, C , is the heat capacity, $Q = Q(x, y, z, t)$ is the internal thermal energy by unit of volume, q_x, q_y and q_z are, respectively, the surface heat flux units along the x, y and z directions.

We can define like this, the thermal fluxes according to the directions of the axes x, y and z according to the Fourier law:

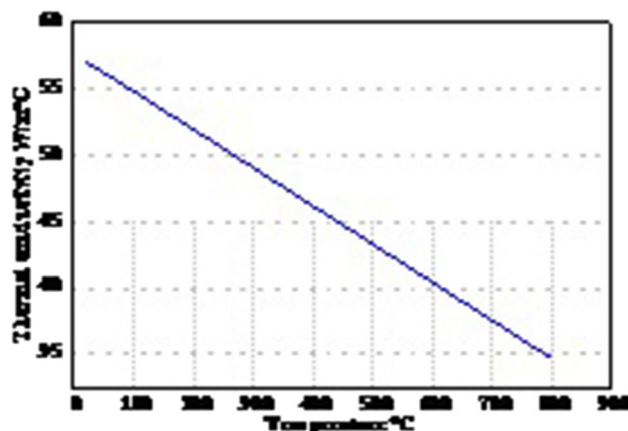


Fig. 13 Thermal conductivity versus temperature [35]

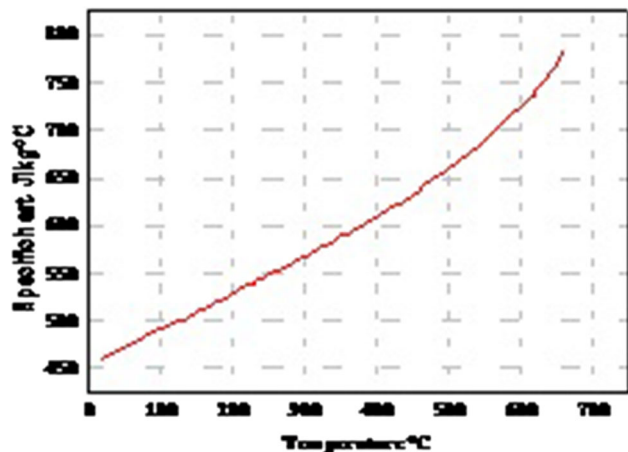


Fig. 14 Specific heat capacity versus temperature [35]

$$\begin{cases} q_x = -k \frac{\partial T}{\partial x} \\ q_y = -k \frac{\partial T}{\partial y} \\ q_z = -k \frac{\partial T}{\partial z} \end{cases} \quad (\text{Eq 8})$$

where k is the thermal conductivity. By substituting Eq 8 in Eq 7, we obtain the following differential equation, which varies as function of temperature T

$$\frac{\partial}{\partial x} \left(k \frac{\partial T}{\partial x} \right) + \frac{\partial}{\partial y} \left(k \frac{\partial T}{\partial y} \right) + \frac{\partial}{\partial z} \left(k \frac{\partial T}{\partial z} \right) + Q + \rho c \frac{\partial T}{\partial t} dx dy dz = 0 \quad (\text{Eq 9})$$

The boundary conditions imposed on our thermal problem are expressed as follows:

- Temperature of fluid that enters the domain is based on the value specified temperature.

$$T_S = T_1(x, y, z, t) \text{ on } S_1 \tag{Eq 10}$$

- Heat flux is controlled by the temperature gradient and always flows from high temperature regions to lower temperature regions.

$$q_x n_x + q_y n_y + q_z n_z = -q_s \text{ on } S_2 \tag{Eq 11}$$

- Convection is group of thermal boundary conditions in which heat flow is a function of convection

$$q_x n_x + q_y n_y + q_z n_z = -h(T_s - T_e) \text{ on } S_3 \tag{Eq 12}$$

where h is the convective exchange coefficient; T_e is the convection surface temperature, and T_s is temperature unknown to the S area. Knowledge of the initial temperature field at the time ($t = 0$) for any transient modeling is mandatory.

$$T(x, y, z, 0) = T_0(x, y, z) \tag{Eq 13}$$

Thermal Loading Applied to the Disc

In this research work, we carried out numerical modeling of the transient thermal transfer in disc brake, by finite element method in which the type of braking of the adopted vehicle is that of emergency stop braking. The speed of the vehicle decreases linearly as a function of time until the moment of braking ($t = 3.5$ s), stabilizing at the value zero until the end of this braking at the instant ($t = 45$ s), as shown in Fig. 15. During the experiment, the disc brake surface temperature, brake pressure, rotor velocity and braking time were measured. Thermocouples provide a

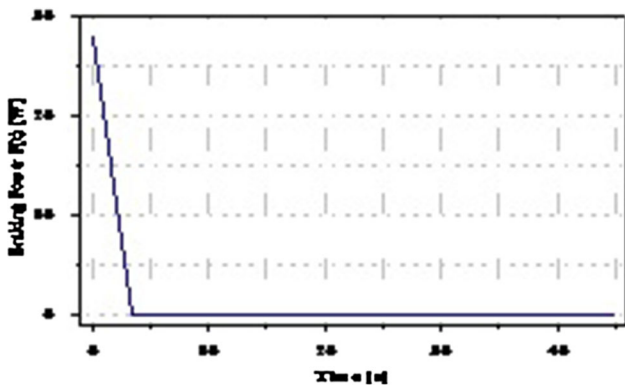


Fig. 15 Braking power versus time

rapid response and can be obtained to suit the particular temperature range. Special consideration of comparison for the maximum temperature in service should be made for cases of the short braking time interval.

This test consists of one braking to a stop, from an initial velocity, of 28 m/s to stop, with a constant deceleration. Total time of this step was 45 s as the time of experimental braking tests. As this phase of the testing was carried out to evaluate the thermal performance of the braking system, it was important that all the tests were performed under similar initial conditions. Prior to any testing, the braking system was put through a number of heating and cooling cycles. This ensured that the residual heat in the brake and thermally linked components was similar for the start of each test.

The heat flux is identified here as the thermal load which is generated by dry friction between the brake disc and the pads during the braking phase. At first, the value of this flow is maximum and it then decreases linearly until it vanishes at the end, as shown in Fig. 16.

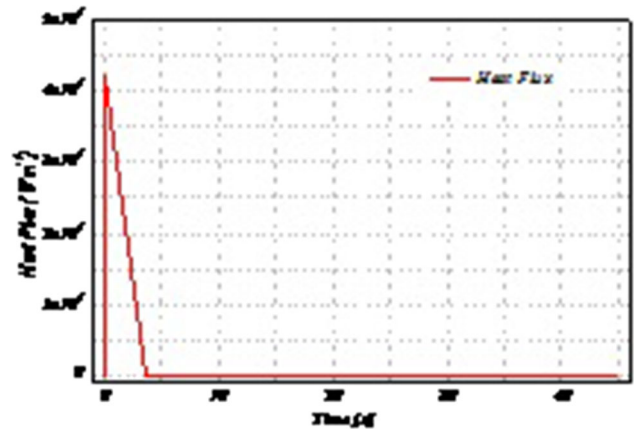


Fig. 16 Heat flux versus time

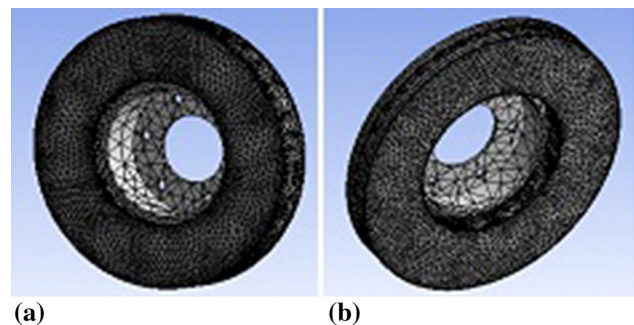


Fig. 17 Disc brake mesh model: (a) full disc, (b) ventilated disc

Mesh of Disc Brake Model

The application of generated mesh of brake disc in numerical modeling is useful from which one has chosen automatic mesh generation. It should be kept in mind that mesh too fine will require very long calculation times and thus increase the final cost to the engineer. Taking into account all this, a fine mesh was chosen to visualize the variations of temperature and heat flow. Thus, the results obtained are more precise. On both brake disc friction tracks where the brake pads are turning, refined tetrahedral mesh has been performed on the ANSYS Multiphysics.

The final mesh, therefore, comprises 172,103 nodes and 114,421 elements for the full disc, and 154,679 nodes and 94,117 elements for the ventilated disc, as it is represented in Fig. 17.

Boundary Conditions Applied to the Model

As thermal analysis is done, the conditions to be taken into account are those that will influence the thermal phenomena such as ambient temperature and that of the fluid. The objective of this study is to perform thermal analysis of brake disc using the ANSYS Workbench software while selecting transient thermal analysis by injecting all the thermomechanical properties of the materials used in the analysis, such as the disc and the brake pads. We introduce the associated boundary conditions for each disc area.

Modeling requires discretization of the time axis. Unlike numerical control, the discretization of the time axis does not have to be regular. The parameters of the initial, minimum and maximum and final time increment for the simulation shall be inserted at the values (0.25, 0.125, 0.5, 45 s), respectively, maintaining the initial temperature of the disc at 20 °C. The thermophysical characteristics of the 3 types of gray cast iron brake discs (FG 15, FG20, and FG25AL) are introduced in the simulation. The values of the convection exchange coefficient (h) for each face of the brake disc must be imported from CFX analysis results and must be used in the ANSYS Workbench Multiphysics analysis. These are shown in the following in the graphs of Fig. 22. The imposed heat flux on the lateral surfaces

corresponds to their values resulting from the CFX analysis.

Solution Procedure of FE Analysis

ANSYS Workbench is a powerful platform that allows you to perform all the steps of the simulation using the finite element method in single interface and to connect the different modules and associated physics (fluids, thermal, structure...). The direct interfacing of ANSYS Workbench with CAD makes it possible to transfer the geometries without risk of errors and to take full advantage of the synergy between the simulation software and the CAD before access to the ANSYS Design Modeler, and the ANSYS Multiphysics (Fig. 18).

Results and Discussion of CFD Analysis

Steady-State Cases

The results obtained from the distribution of the wall heat transfer coefficient of the two brake discs in the steady-state case are illustrated in Figs. 19 and 20.

Table 4 lists the average heat transfer coefficients of the named surfaces in the CFD model of the full brake disc made of the material FG15.

The distribution of the heat transfer coefficient to the wall (h) according to the three types of brake disc materials is well represented in Fig. 20a, b, and c. It is observed that the variation of (h) in the brake disc does not subordinate to the material and that this one is not the same one found in the specialized literature.

From the maximum and minimum values of the various areas of the ventilated brake disc, the average values of the heat transfer coefficient can be taken from the wall (h). These harvested data are grouped in Table 5. From the observation, it can be seen that there is no significant variation in this coefficient (h) when changing the material of the brake disc. Contrary to what we have seen, the heat transfer coefficient values at the wall are much more influenced by the ventilation system of the brake disc for the same material (FG15).

The velocity contour is plotted in Fig. 21. The velocity vector shows the direction of fluid particles over the disc surface with vanes. The velocity is higher at the leading edge of the ventilated disc brake. Higher pumping effect is noticed in the velocity distribution. The distribution of the fluid velocity is well observed non-homogeneous and it is random which corresponds in fact to a turbulent flow regime around the ventilated brake disc. The recirculation zones cause flow separation and conjointly it will end in energy loss within the flow. The velocity distribution on the

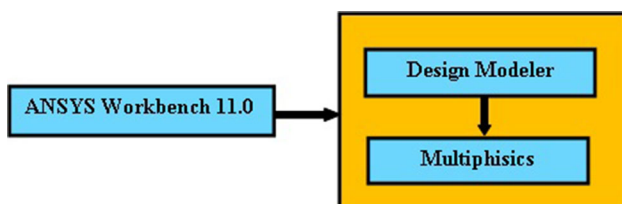
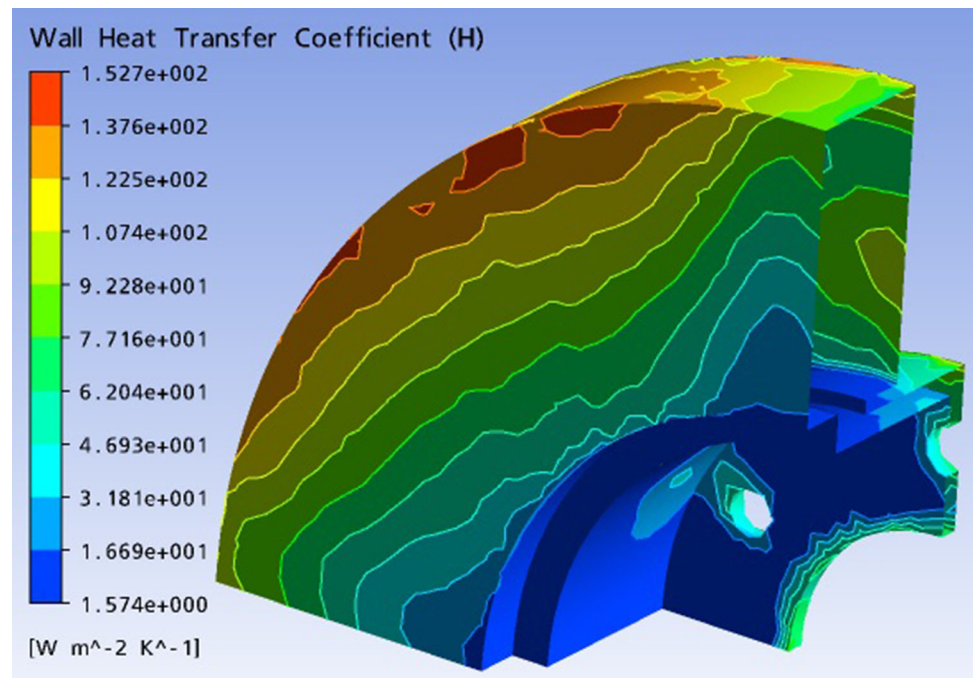


Fig. 18 ANSYS Workbench 11 module

Fig. 19 Values of heat transfer coefficient at the wall of the full disc with material FG15 in steady-state thermal analysis



vane surface channels (channels) in the ventilated brake disc of the vehicle is well marked using CFX Pre software whose speed is low just at the exit of the disc at vanes.

Transient Cases

Evaluation of the Heat Exchange Coefficient (h)

Heat transfer coefficient of the wall (h) is a physical quantity which is related to the geometric design of the brake disc, the velocity of the air circulation, as well as other parameters attached to the braking process. Indeed, when the vehicle moves in motion, the heat exchange coefficient (h) in the company of air changes with the speed of the disc, it depends on the form of braking medium. In transient situation, this convective heat exchange coefficient (h) is variable as function of time on each disc surface [36]. This one, practically, has nothing to do with the material, but, it depends on the surface geometry as well as the conditions of law of the convective regime.

Figure 22a and b shows the evolution of the heat transfer coefficient (h) at each surface of the full and ventilated disc, as function of time. We used these two graphs later to predict the three-dimensional distribution of the two brake discs. It can be said that the values of the convective heat exchange coefficient (h) vary according to the geometric design of the disc, whether it is full or ventilated and, it is quite rational that the aeration generates the decrease in the maximum temperatures at the walls. The variations of the wall heat transfer coefficient as

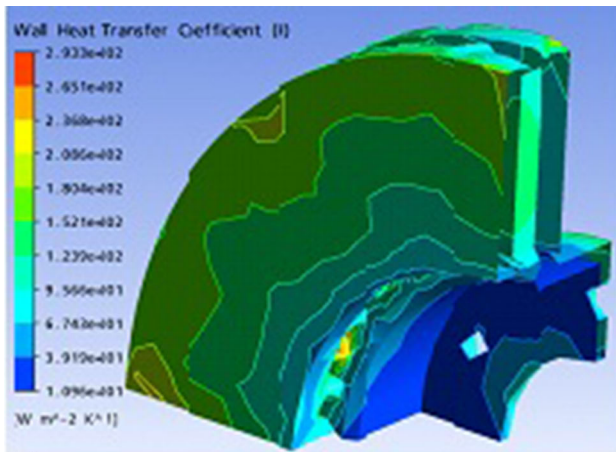
function of time for insulated surfaces SV1 and SPV2, respectively, belong to the full and ventilated brake disc for material FG15 are clearly shown in Fig. 23a and b.

Results and Discussion of Thermal Analysis

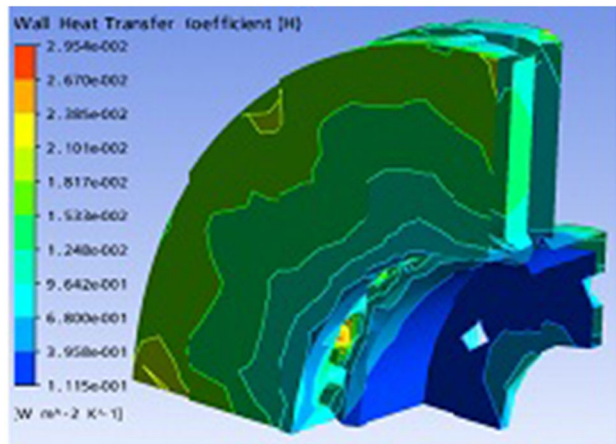
Results of the Disc Temperature

In order to perform multi-step analysis, and to simulate the thermal behavior of full and ventilated disc brake, we used the ANSYS Workbench 11.0 software during the transient thermal analysis. The inner and outer faces of the brake disc are designed to generate symmetrical heat flow upon mutual sliding of the disc when it is rotated around the brake pads. During this cyclic mechanism, we distinguish the alternation of two thermal phenomena associated with convection; it is in this case, the heating and cooling of the brake disc.

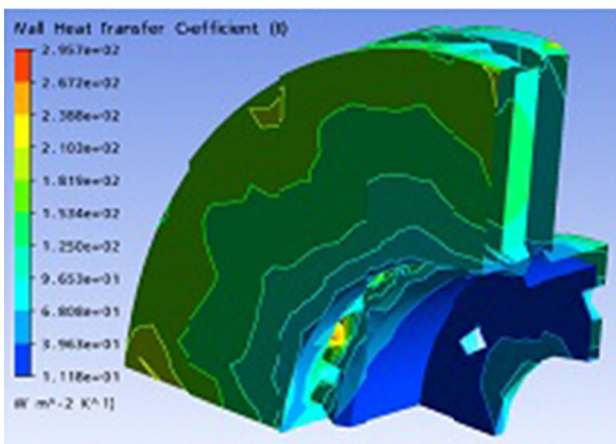
The transient thermal analysis of the two discs, full and ventilated brake discs were performed using finite element (FE) software. The calculation does not last very long, which is positive point. The results of the temperature distribution (3D) for the three materials, namely the gray cast iron FG25AL, FG20, and FG15 are provided in Fig. 24. It should be understood that the material having lower thermal conductivity thus generates important thermal gradients and consequently increase in the surface temperature of the brake disc. We recall here that convection is a mode of heat dissipation that it is not



(a)



(b)



(c)

Fig. 20 Values of heat transfer coefficient at the wall of the ventilated discs with materials (a) FG25 AL, (b) FG20 and (c) FG15 in steady-state thermal analysis

influenced by the material but it is related to the hot body design. So brake rotor material choice depends on the material thermal conductivity and the specific heat capacity, whereas the rotor cooling depends on the rotor design.

Table 4 Values of the wall heat transfer coefficients of different surfaces in the steady-state case for full disc with material FG15

Surface	Material FG15 $h_{average} = (W/m^2 k)$
SC1	25.29168
SC2	5.18003
SC3	2.922075
SC4	11.77396
SF1	111.20765
SF3	53.15547
ST2	23.22845
ST3	65.6994
ST4	44.26725
SV1	81.37535
SV2	71.75842
SV3	41.83303
SV4	65.82545

Table 5 Values of the wall heat transfer coefficients of different surfaces in steady-state case for ventilated discs with materials FG25 AL, FG20 and FG15

Materials Surface	FG25 AL	FG20 $h_{average} = (W/m^2 k)$	FG15
SC1	54.1624	53.9260	53.8749
SC2	84.6842	83.7842	83.6516
SC3	44.4171	44.3485	44.3295
SF1 and 2	135.4039	135.0584	135.0007
SF3	97.1710	95.0479	94.8256
SPV1	170.6472	171.4507	171.5696
SPV2	134.0815	134.3285	134.3615
SPV3	191.2441	191.9436	192.0391
SPV4	175.1667	176.13340	176.2763
ST1	113.6098	114.3962	114.3916
ST2	35.0993	34.4723	34.3473
sST3	68.3316	66.3316	66.0317
ST4	75.0945	72.1235	71.6642
SV1	135.5299	131.1183	131.2075
SV2	119.2572	118.4648	118.2040
SV3	46.7023	44.8195	44.5264
SV4	111.5769	108.5044	108.1817

From the results provided by this simulation, it can be seen that the ventilated discs made of the materials FG20 and FG25AL, respectively, having temperatures reaching 351.5 and 380.2 °C, which in turn, are greater than that of the ventilated disc of material FG15 having a maximum temperature of 345.4 °C as indicated in Fig. 25. It can thus be concluded that the most suitable material in this case for

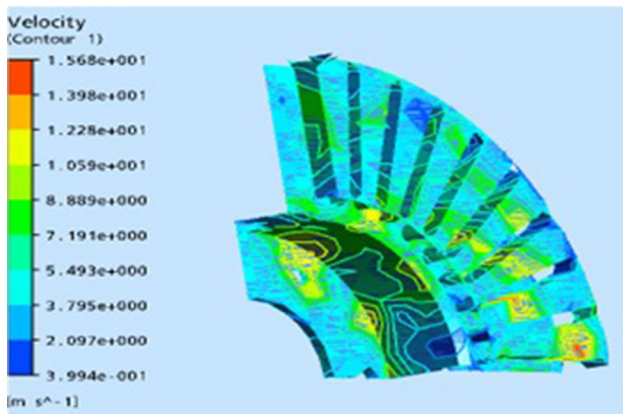


Fig. 21 Velocity contour of ventilated disc rotor

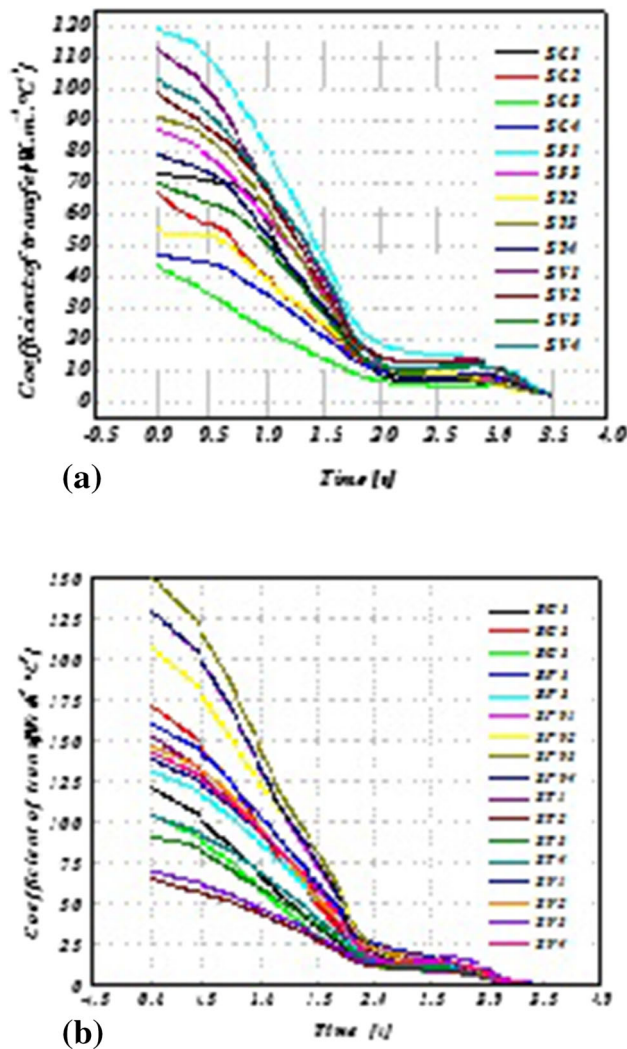


Fig. 22 Heat transfer coefficient (h) versus time at different disc surfaces at material FG15 in transient thermal case for (a) full disc faces, and (b) ventilated disc

the brake discs is the gray cast iron FG15 which presents the better thermal performance.

Figure 26 shows the temperature of the brake disc at time $t = 1.8$ s reaching the maximum value of $401.5\text{ }^\circ\text{C}$, and after that, it decreases exponentially at 4.9 s until it reaches braking cycle termination at instant, $t = 45$ s. The forced convection step is well designated in the temporary interval between the instant 0 s and 3.5 s, as shown in Fig. 26. On the other hand, the natural or free convection is quite marked after the duration of the forced convection arriving at the end of braking time, which is the total time of the simulation ($t = 45$ s). It can be seen from the graphs that the temperature of the full brake disc exceeds that of the ventilated disc with difference of $60\text{ }^\circ\text{C}$. Finally, we can draw the conclusion that the ventilated brake disc allows us to provide better cooling therefore, better endurance and gives us ability to dissipate more heat for braking efficiency.

Thermomechanical Coupling Analysis

Calculation of Hydraulic Pressure

In order to proceed with the preliminary mechanical calculation, we determined the constant value of the hydraulic pressure exerted by the piston on the inner brake pad. For this, we assumed that the rate of 60% of the braking forces is maintained both front brake discs, giving a percentage of 30% for each rotor [37]. So, using the data in Table 6, we can thus calculate the typical force of a single rotor as follows (see Annex B for more detail)

$$F_{\text{disc}} = \frac{(30\%) \frac{1}{2} m v_0^2}{2 \frac{R_{\text{rotor}}}{R_{\text{tire}}} \left(v_0 t_{\text{stop}} - \frac{1}{2} \left\{ \frac{v_0}{t_{\text{stop}}} \right\} t_{\text{stop}}^2 \right)} = 1047.36 \text{ (N)} \tag{Eq 14}$$

The angular velocity of the rotor can be evaluated as follows

$$\omega = \frac{v_0}{R_{\text{tire}}} = 157.89 \text{ rad/s} \tag{Eq 15}$$

We used ANSYS Workbench software to determine the entire area of the disc friction track swept by the brake pads during rotation while selecting on this contact surface that is equal to $35,797\text{ mm}^2$, as it is shown in green color in Fig. 27.

Using the above calculations, the value of the hydraulic pressure P is obtained from the following form [38]

$$P = \frac{F_{\text{disc}}}{A_c \mu} = 1 \text{ (MPa)} \tag{Eq 16}$$

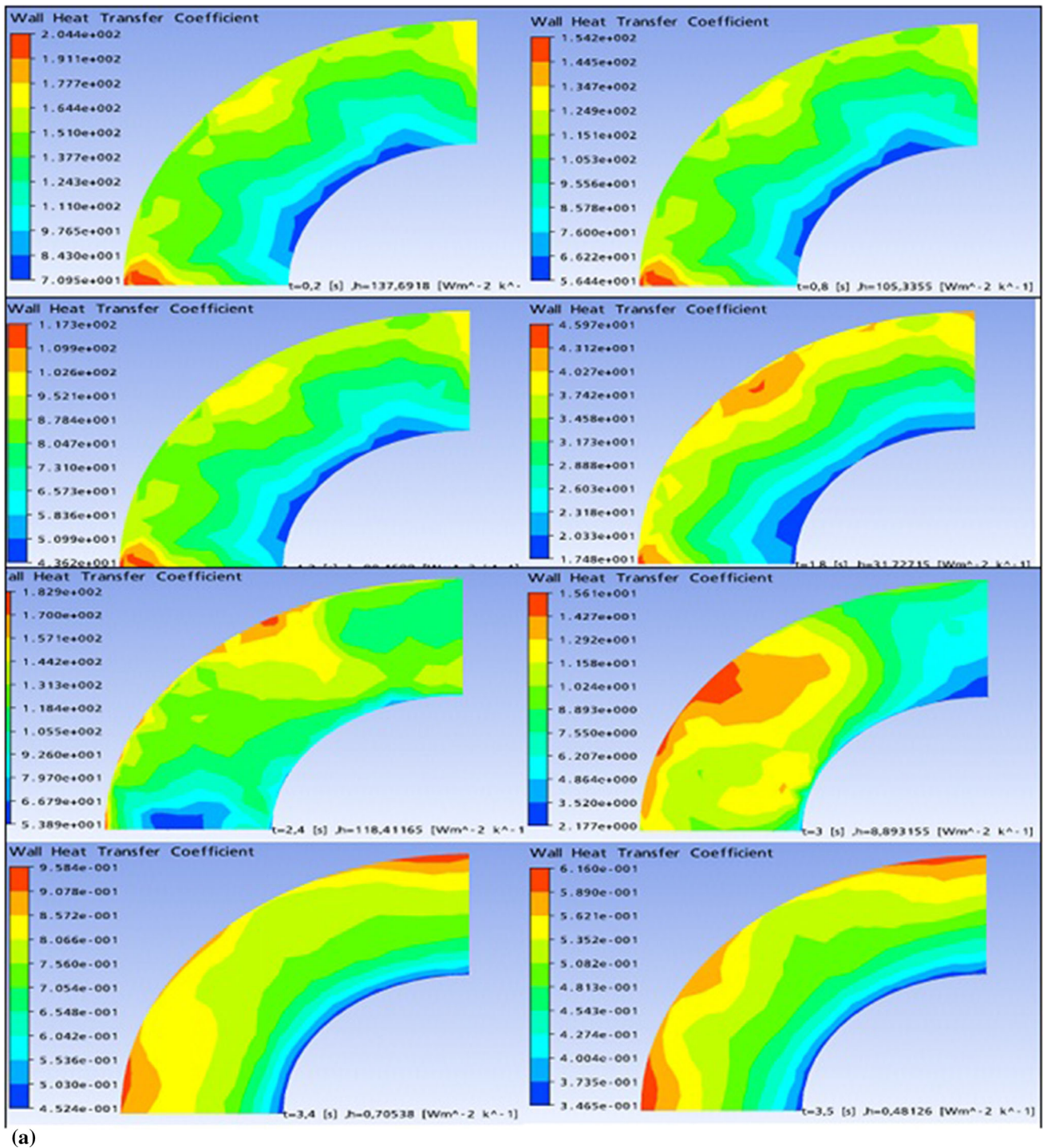


Fig. 23 Variation of the heat transfer coefficients (h) in specific time sequence of the discs with FG15 material (a) surface SV1 of the full disc and (b) surface SV2 of the ventilated disc

where μ , is the friction coefficient, A_c is the surface of the brake pad in contact with the brake disc, which is obtained directly from simple selection in ANSYS Workbench. In

our case, it is indicated in green in Fig. 28 and equal to 5246.3 mm^2 .

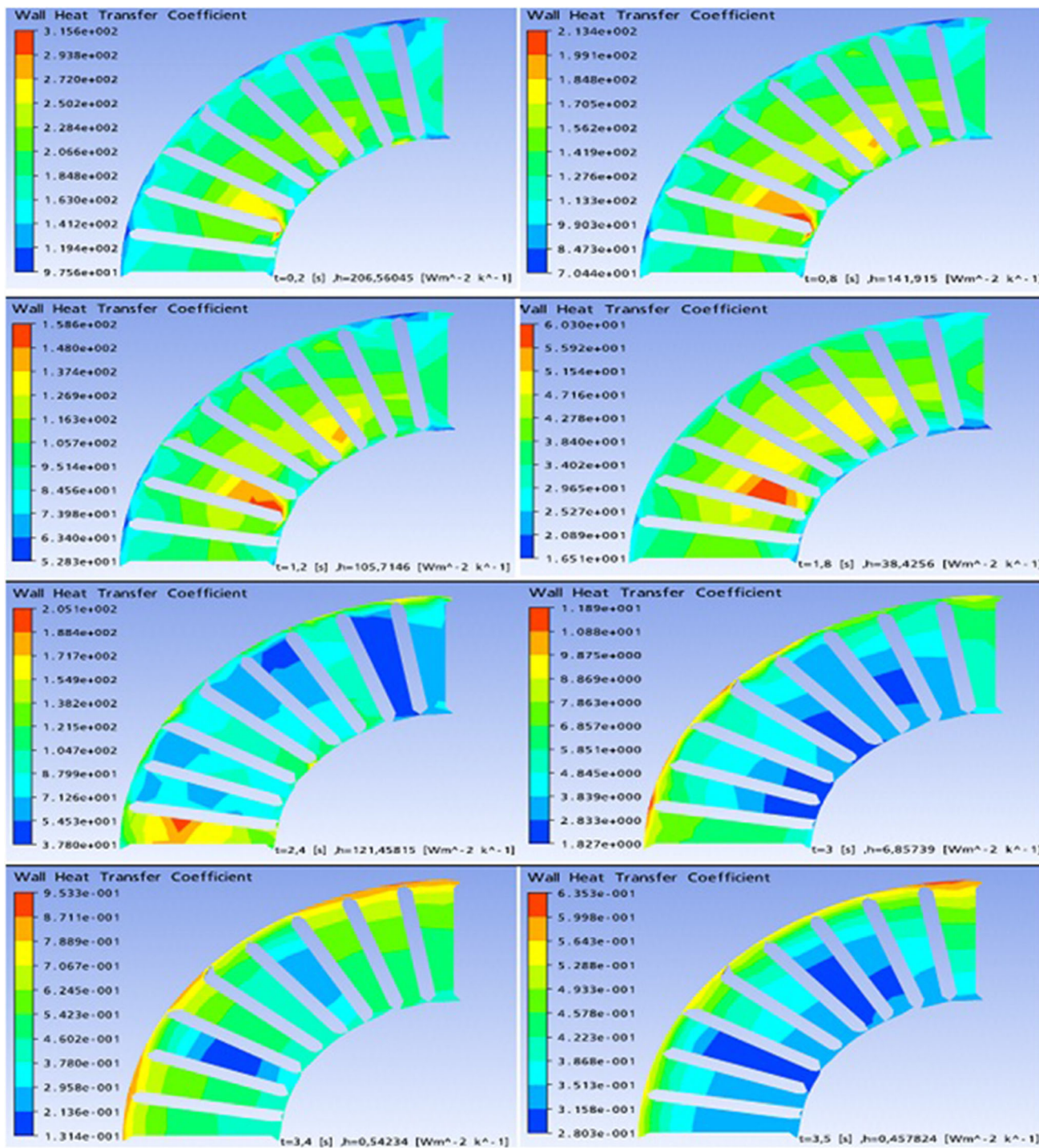


Fig. 23 continued

Elastic Problem

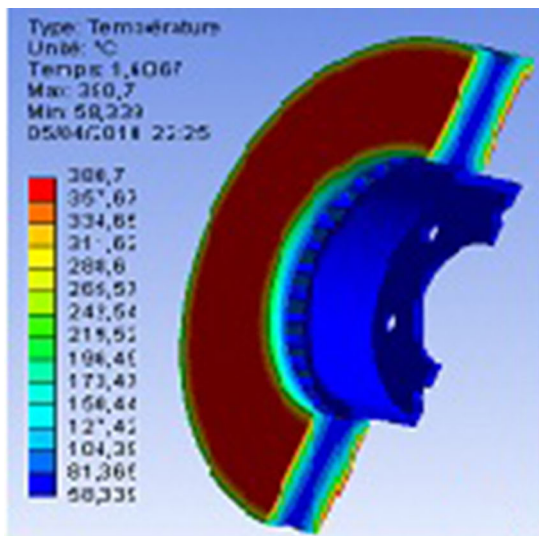
The mechanical stress is linked to the effort by a constitutive equation following:

$$\{\sigma\} = [D] \{\epsilon^{me}\} \tag{Eq 17}$$

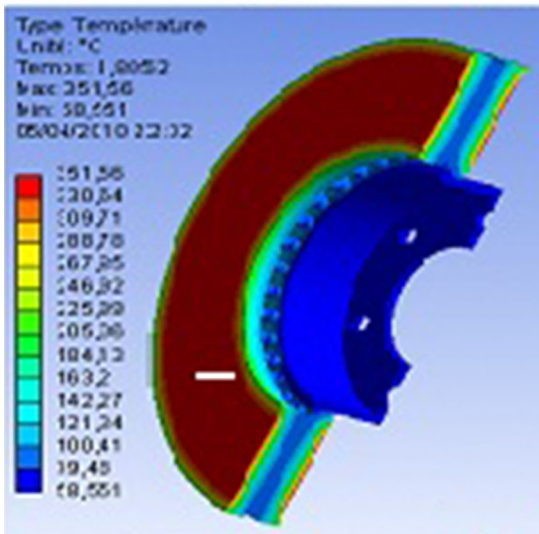
where $[D]$ is the material property matrix.

The total stress, sum of the mechanical and thermal stresses, is given by:

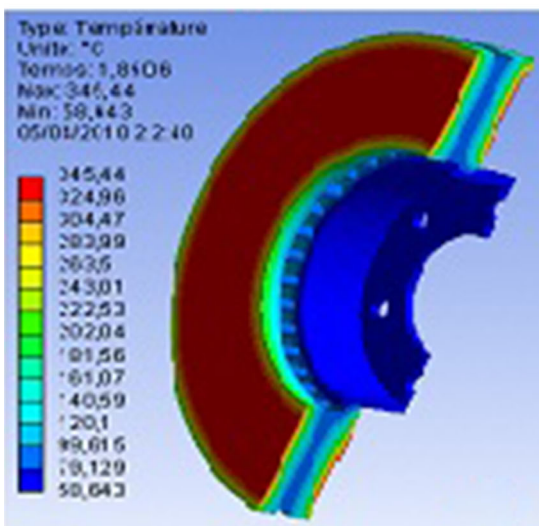
$$\{\epsilon\} = \{\epsilon^{me}\} + \{\epsilon^{th}\} \tag{Eq 18}$$



(a)

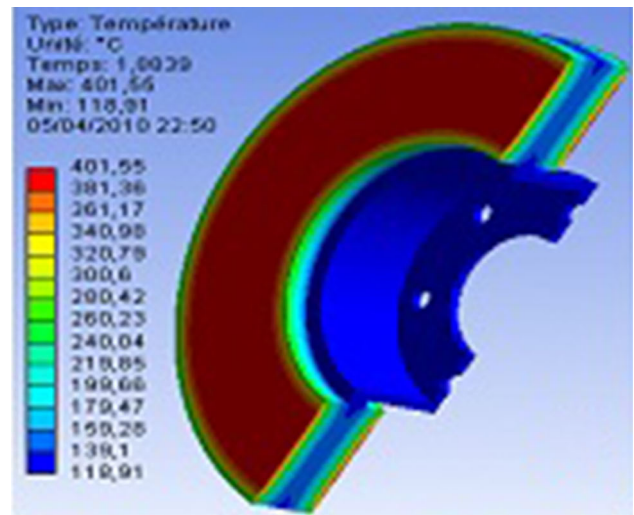


(b)

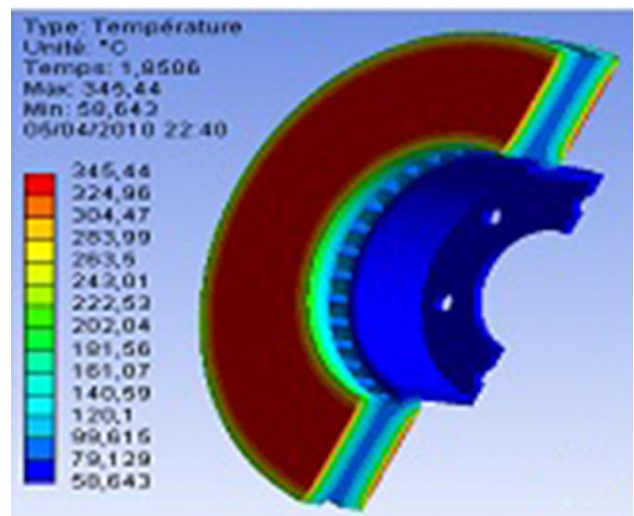


(c)

◀Fig. 24 Temperature plot of ventilated discs for three materials gray cast iron (a) FG25 AL, (b) FG20, and (c) FG15



(a)



(b)

Fig. 25 Temperature plot on disc brake of the same material (FG15) (a) full disc, (b) ventilated disc

where the upper indices (me) and (th) denote mechanical and thermal stresses, respectively.

Equation (17) becomes:

$$\{\sigma\} = [D]\{\{\varepsilon\} - \{\varepsilon^{th}\}\} \tag{Eq 19}$$

where $\{\sigma\} = \{\sigma_r, \sigma_\theta, \sigma_z, \sigma_{r\theta}, \sigma_{\theta z}, \sigma_{zr}\}$, $\{\varepsilon\} = \{\varepsilon_r, \varepsilon_\theta, \varepsilon_z, \varepsilon_{r\theta}, \varepsilon_{\theta z}, \varepsilon_{zr}\}$.

For isotropic material, temperature change results in body expansion or shrinkage but no deformation. In other

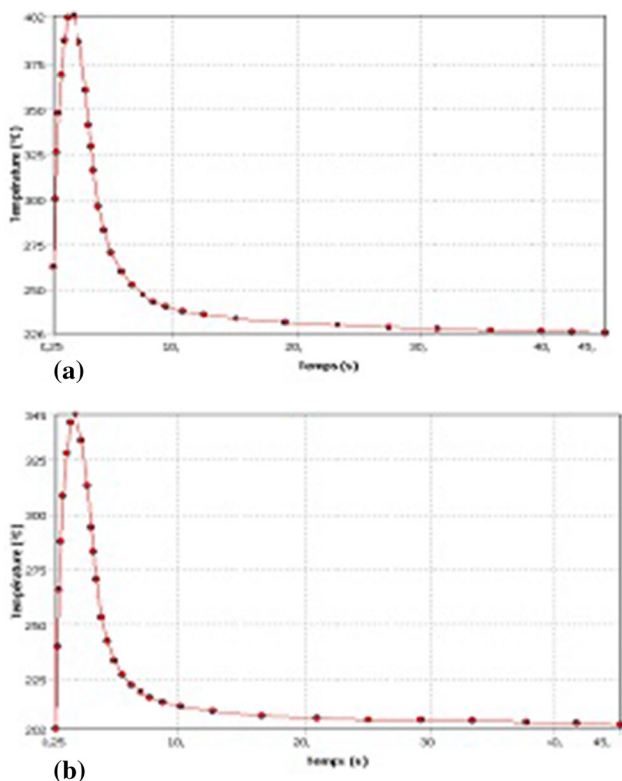


Fig. 26 Disc temperature versus time for (a) full disc and (b) ventilated disc, for material gray cast iron FG15

Table 6 Vehicle data

Item	Value
Vehicle mass— m (kg)	1385
The initial velocity— v_0 (m/s)	60
Duration of braking application— t_{stop} (s)	45
The effective radius of the disc (mm)	100.5
The radius of the wheel (mm)	380
Friction coefficient disc/pad μ	0.2
Pad surface A_c (mm ²)	5246.3

words, the temperature change affects the normal stresses without shear stresses.

The thermal stress vector is expressed as follows:

$$\{\epsilon^{th}\} = \{\alpha\Delta T \ \alpha\Delta T \ \alpha\Delta T \ 0 \ 0 \ 0\}$$

which α , is the coefficient of thermal expansion and ΔT indicates the temperature difference. Total stress is expressed in terms of nodal displacements as

$$\{\epsilon\} = [B]\{d\} \tag{Eq 20}$$

where $[B]$ is the kinematic matrix.

Substitute (20) in (19), we will have:

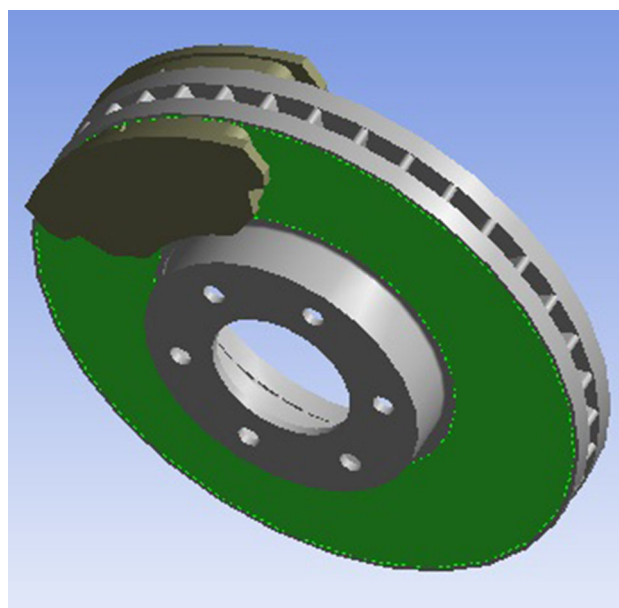


Fig. 27 Contact surface of the disc

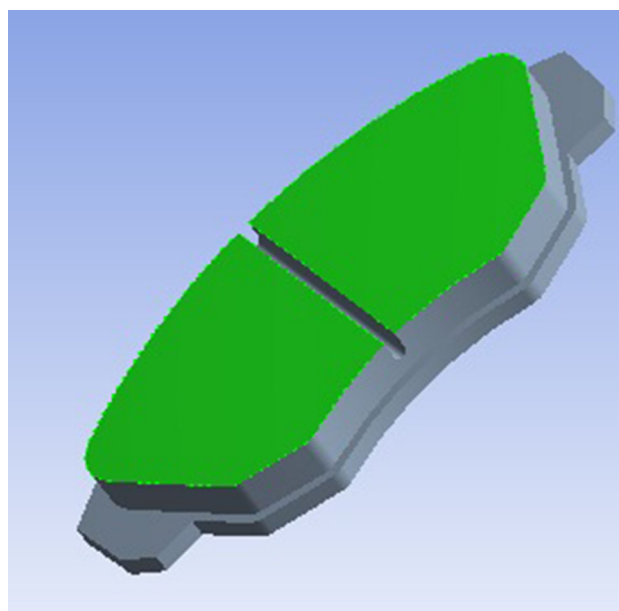


Fig. 28 Contact surface of the pad

$$\{\sigma\} = [D][B]\{d\} - [D]\{\epsilon^{th}\} \tag{Eq 21}$$

The weighted residual method is applied to Eq 21 and the results are found in the following equation

$$[K]\{d\} = \{F^{th}\} + \{F^{me}\} \tag{Eq 22}$$

where the elemental stiffness matrix for elasticity is given in the form:

$$[K^e] = \int_{\Omega^e} [B]^T [D] [B] d\Omega \tag{Eq 23}$$

$\{F^{th}\}$ and $\{F^{me}\}$ are the thermal and mechanical force vectors that are denoted as follows:

$$\{F^{th}\} = \int_{\Omega} N^T N d\Omega$$

$$\{F^{me}\} = \int_s N^T N dS$$

The elastic problem is solved by employing the constitutive equation. During numerical modeling, special attention is required to satisfy the continuity of normal displacements on the contact surface and the overlap conditions [39].

The following conditions of movement and effort are imposed on each pair of nodes on the interface

$$W_i = W_j \text{ when } P > 0; W_i \neq W_j \text{ everywhere} \tag{Eq 24}$$

$$\sigma_{zj} = -\sigma_{zj} \text{ when } P > 0; \sigma_{zj} \neq \sigma_{zj} \text{ everywhere} \tag{Eq 25}$$

The following conditions of temperature and heat flux constraints are imposed on each pair of nodes on the interface

$$T_i = T_j \text{ when } P > 0; T_i \neq T_j \text{ everywhere} \tag{Eq 26}$$

$$q^* = \mu P \omega r \text{ when } P > 0; q^* = 0 \text{ everywhere} \tag{Eq 27}$$

FE Model and Boundary Conditions

The boundary conditions applied to the model result from the assumptions and model choices presented above. Figure 29a and b shows the boundary conditions imposed on FE model, consisting of the brake disc and two brake pads in dry contact in the case of pressure exerted on one side of the pad and that of double pressure on both sides of the pad.

As we have done thermal analysis, the conditions to be taken into account are those which will influence the thermal phenomena such as the ambient temperature which is the initial temperature of disc 20 °C, the thermal flow and that of convection imposed on all the surfaces of the

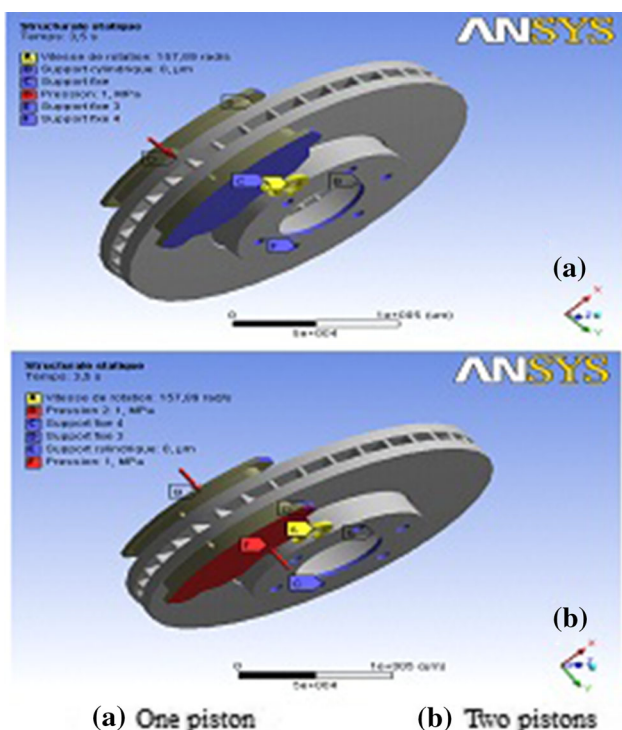


Fig. 29 Loading conditions for disc brake assembly. (a) One piston, (b) two pistons

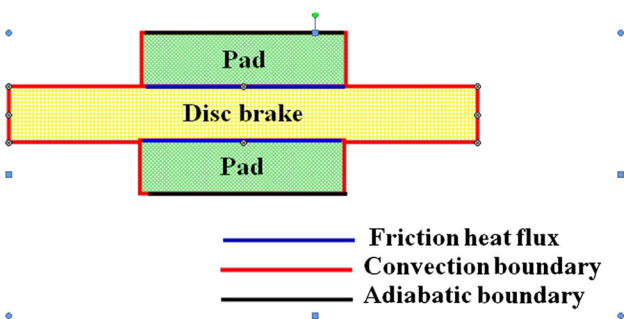


Fig. 30 Thermal boundary condition applied to the model

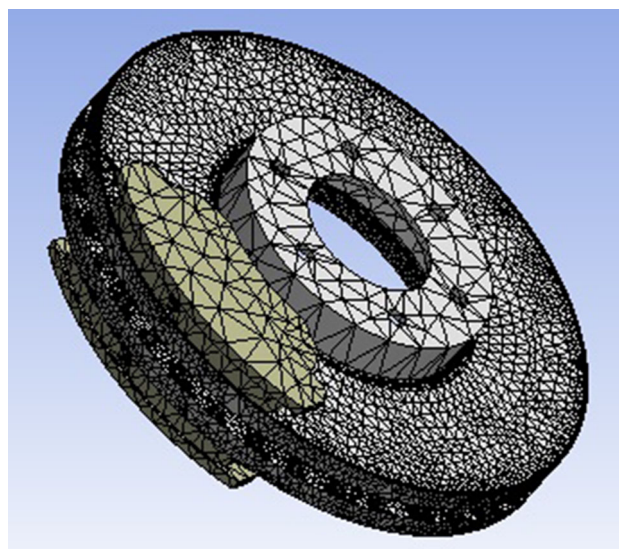


Fig. 31 Meshed model of disc brake assembly

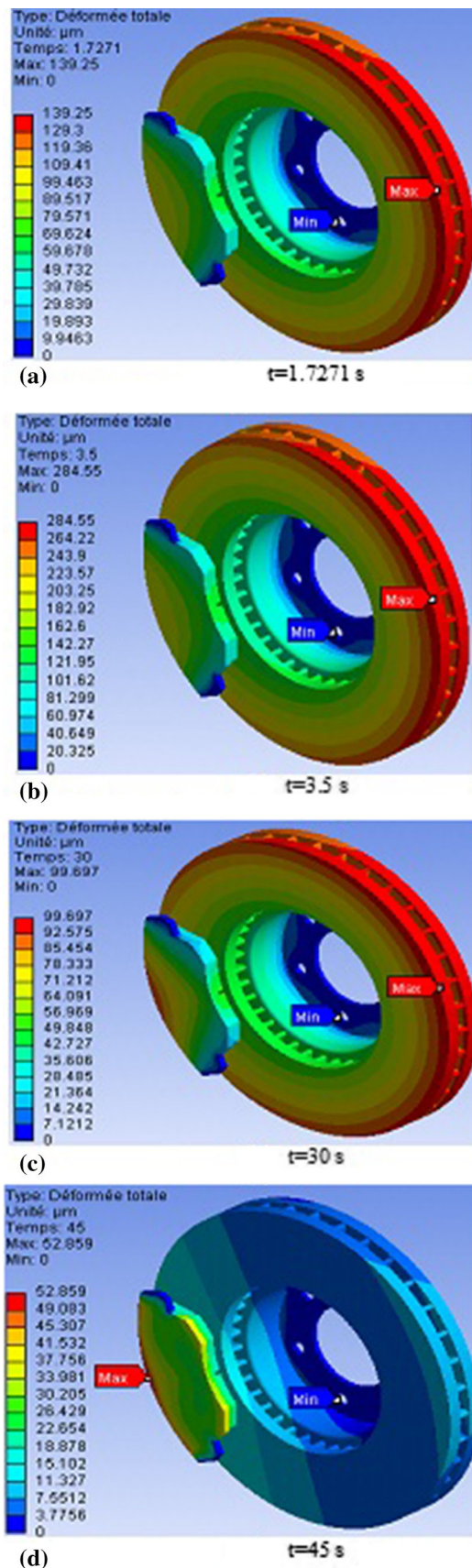


Fig. 32 Total deformation of disc-pad model. (a) $t = 1.7271$ s, (b) $t = 3.5$ s, (c) $t = 30$ s, (d) $t = 45$ s

brake disc while for the two brake pads [40], convective heat exchange coefficient (h) of value $5 \text{ W/m}^2 \text{ }^\circ\text{C}$ is applied on their outer surfaces on both sides (Fig. 30).

For structural boundary conditions, we know that the brake disc is fixed to the mounting holes thus requiring fixed support on these holes taking into account its rotational speed [39] $\omega = 157.89 \text{ rad/s}$. The internal disc diameter is sustained at fixed support for both radial directions while the tangential direction is left free in this simulation.

The structural boundary conditions applied to pads are also introduced. Uniform contact pressure distribution was assumed. Constant value of the friction coefficient in the entire course of the brake application was assumed. We imposed pressure of 1 MPa on the piston pad while maintaining fixed support on the finger pad while on the contact surface; the pad is assembled on its edges at the perpendicular plane. The friction between the two parts (disc-brake pad) is defined by a coefficient equal to 0.2.

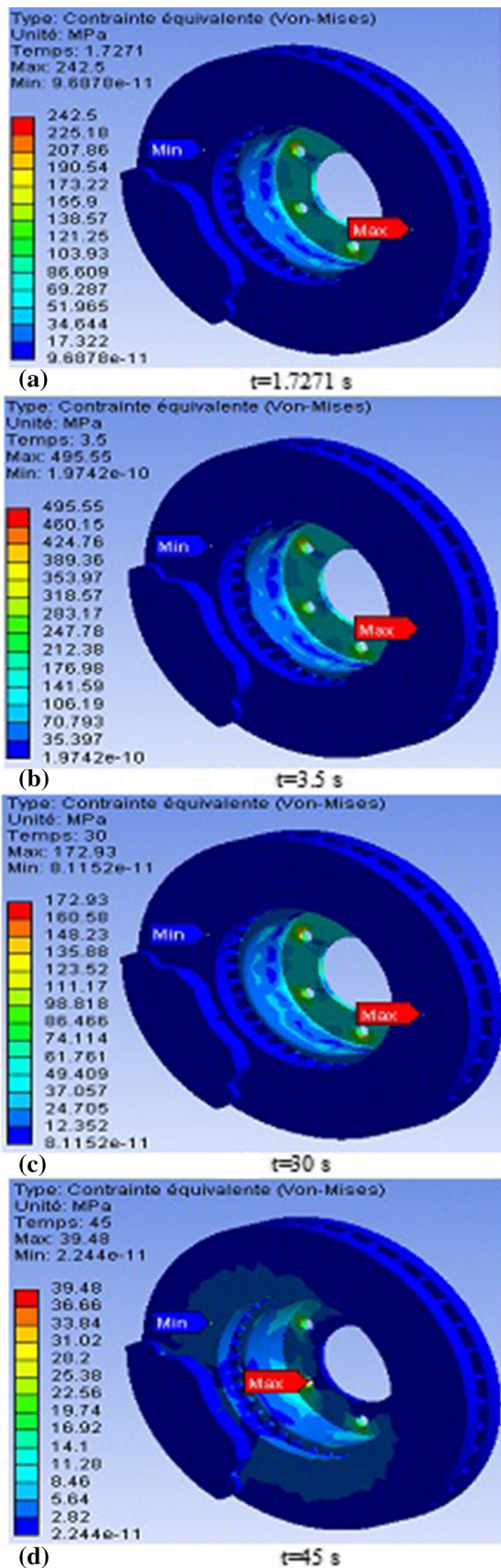
Geometry and Mesh

Three-dimensional mesh of ventilated disc was generated using the ANSYS software (Fig. 31). It is elementary solid respecting the periodicity of the fasteners of the bowl and internal cooling fins, representing entire disc. The brake disc is divided into two volumes to allow refinement of the mesh of the friction tracks. The first volume consists of two friction tracks. The mesh is three-dimensional (3D) tetrahedral type with 10 nodes, regular on the friction tracks and more fine as when approaching the friction surfaces. The second volume consists of the remaining disc with the bowl and the internal cooling fins. The total number of nodes is 185,901 while the total number of elements is 113,367.

Results and Discussion of Thermo-structural Analysis

Thermal Distortion

The pressure distribution and the actual contact area vary as long as there is thermal deformation during the braking process. The mechanical and thermal deformations overlap with each other as whole from which the deformation of the disc has become very large in its circumference and decreases gently in its radial direction, of which this is well exposed in its lateral section because of the presence of thermal loading. Indeed, frictional heating causes non-



◀**Fig. 33** von Mises equivalent stress obtained step by step. (a) $t = 1.7271$ s, (b) $t = 3.5$ s, (c) $t = 30$ s, (d) $t = 45$ s

uniform pressure distribution between the brake pads and the brake disc which causes its thermal deformation. In other words, the deformation of the brake disc area is mainly due to the thermal expansion of the brake disc material.

Figure 32 shows the maps of the total deformation of the whole model (disc-brake pads) evaluated at times $t = 1.7271, 3.5, 30$ and 45 s. According to this figure, the maximum total deformation recorded at time $t = 3.5$ s is of the order of $284.55 \mu\text{m}$, where it coincides with the braking moment. It is obvious that strong distribution amplifies with time as well on the friction tracks of the disc and its outer ring that its fins of cooling. Indeed, at the beginning of the braking, relatively homogeneous, hotspots appear on the friction tracks of the disc. During braking, this hot strip with hot spots gradually migrates to the inner radius. Hot spots intensify to form stationary macroscopic spots at the inner radius. At the end of the braking, the intensity decreases and the surface gradients homogenize. The migration of the locations is explained by the difference in expansion between the track of the disc and its rear face, leading to “umbrella” deformed disc during warm-up. Deformation of the structure, therefore, has preponderant role in the migration of thermal locations.

von Mises Stress Distribution

Most disc brakes used in automotive, industry are subjected to thermal loads produced by temperature variations in addition to mechanical loads. The model provides access to von Mises stress distribution mapping at the start of braking (Fig. 33) and after cooling the sector to ambient temperature. The von Mises stress change here, at the same time in the presence of the temperature and the pressure, because the mechanical stresses resulting from contact pressure adds to the thermal stresses. The application of the internal pressure increases the level of the von Mises stress for all positions and the increase in temperature causes also the increase in these stresses in the brake disc. The distribution is well noted here in order ranging from 0 to 495.56 MPa. The great value recorded during this modeling in the thermomechanical coupling is very significant when compared to the mechanical analysis of dry contact under the same braking conditions. According to the established conclusion, the von Mises stresses are maximums in the outer band at the level of the disc brake bowl at the instant 3.5 s, corresponding to the moment when the thermal gradient in the track thickness is the most

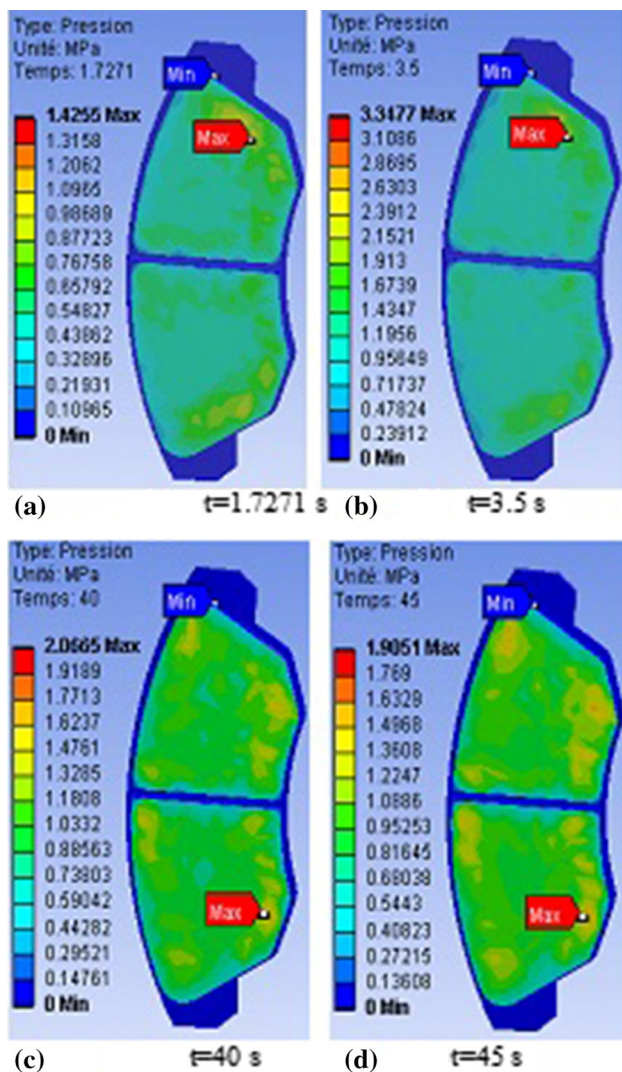


Fig. 34 Contact pressure distribution in the inner pad. (a) $t = 1.7271$ s, (b) $t = 3.5$ s, (c) $t = 40$ s, (d) $t = 45$ s

important. The maximum stress values occur in areas where the disc is in contact with the wheel and shaft. That is where the disc is screwed to the wheel flange and where it is in contact with the shaft. In these areas, the highest values of stresses occur because the wheels and shafts under the force of inertia tend to continue turning until the disc along with the pads and the rest of the brake system does not allow. More precisely, it comes to the appearance of torsion. Indeed, the brake disc is fixed to the hub by bolts in order to prevent its movement and as soon as it starts to rotate, torsion and shear stresses have just been produced at the level of its bowl which generates automatically stress concentrations around its fixing holes. The disc bowl thus risks mechanical rupture under repetitions of these undesirable effects during the braking process. The general evolution of the stresses in the disc during the braking-

cooling cycle is in agreement with the phenomena described in the previous literature searches.

Contact Pressure Distribution

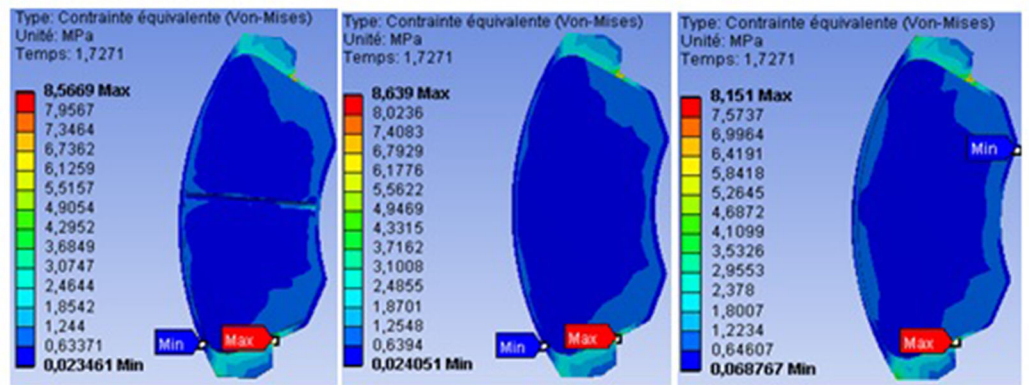
The braking operations are characterized by the sliding speed, the apparent contact pressure, the braking time, the energy dissipated by the brake and the initial braking power. The heat generated on contact and the wave deformation of the disc caused by the differences in thermal expansion lead to the migration of the contact in the form of hot band on the circumference of the disc. Within this hot band, contact pressure and the dissipated energy are very high. The contact is said to be closed in the hot band area and otherwise open. After the passage of the hot band, in the open hot zone, third body debris is observed on the surface of the disc. These powders recirculate in contact with the rotation of the disc.

Figure 34 shows mapping of the contact pressure at the friction interface between the inner brake pad and brake disc with various simulation times. In these, the maximum contact pressures evaluated are of the order of 3.3477 MPa at the instant when the rotational speed is zero $t = 3.5$ s. It can also be seen that this maximum value is in the leading edges of the pads toward the trailing edge by friction. Moreover, the distribution of the contact pressure is quite symmetrical with respect to the groove of the brake pads. In the thermomechanical coupling that we carried out here, it is clear that the contact pressures are not negligible and can reach locally very high values, of the order of GPa. The plastic flow observed in the sliding direction attests well to the severity of the friction forces, so very high contact pressure.

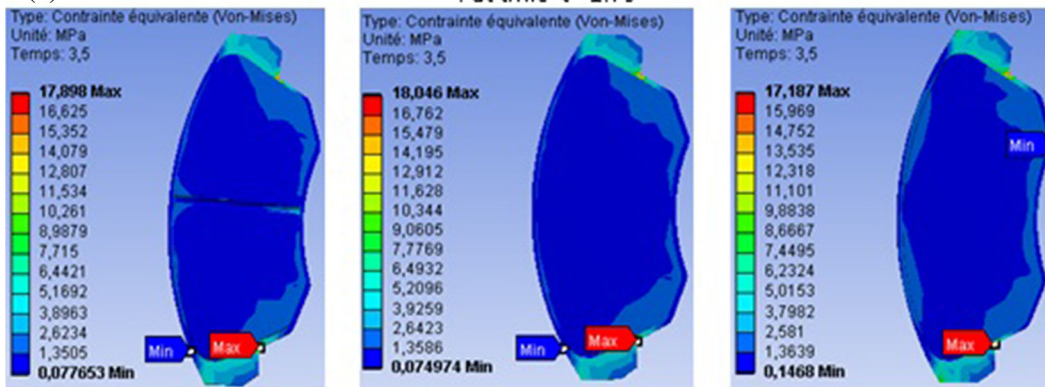
von Mises Stress at Inner Pad

In order to study the influence of the groove of the brake pads as well as loading modes applied to the pistons (single-pressure and double-pressure). We solve the model and ask for the equivalent von Mises stress of three different designs. Brake pads in this case, brake pad with center groove subjects to single double piston. We obtain the following visuals that are grouped in Fig. 35a, b, c, d, e, f, and g. It can be seen that almost all the contact pads of the brake pads are dressed in dark blue color meaning low stresses at the beginning of the braking moment ($t = 1.7$ s).

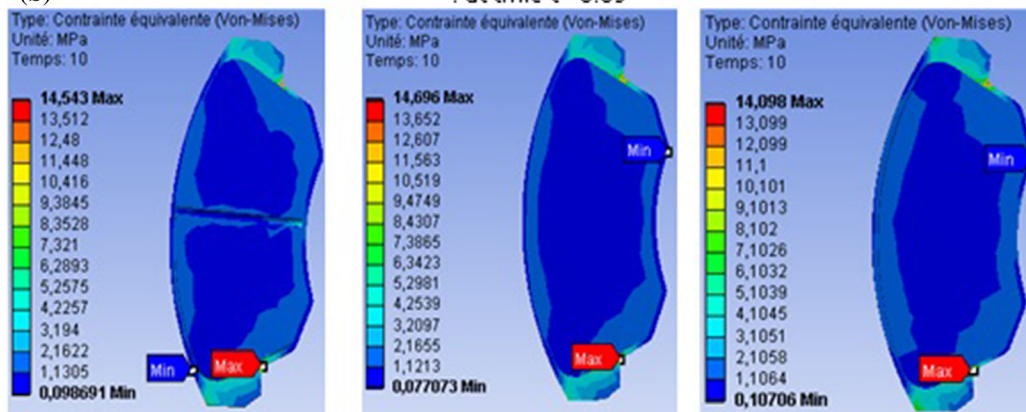
Nevertheless, from the moment of the end of braking $t = 45$ s, the scale of von Mises stress becomes more important whose vision of the colors becomes practically blue ocean whose distribution is well noticed on the three conceptions. We can also see in this figure, symmetrical distribution with respect to the middle of the brake pad for the three designs, and that the von Mises stress of the brake



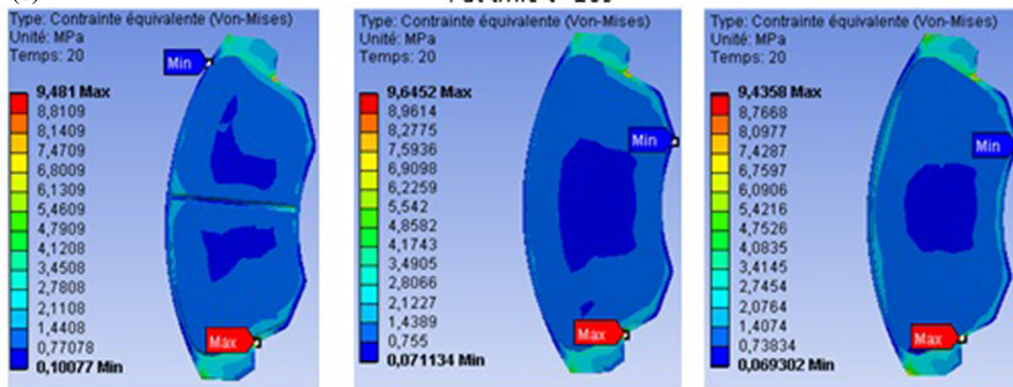
(a) : at time $t = 1.7s$



(b) : at time $t = 3.5s$



(c) : at time $t = 10s$



(d) : at time $t = 20s$

◀ **Fig. 35** Distribution of von Mises stress at different braking times: Single piston with pad center groove (left), Single piston without groove (center) and Double piston without pad groove (right). (a) At time $t = 1.7$ s, (b) at time $t = 3.5$ s, (c) at time $t = 10$ s, (d) at time $t = 20$ s, (e) at time $t = 30$ s, (f) at time $t = 40$ s, (g) at time $t = 45$ s

pads adopted at floating caliper of single piston (left) are significantly lower than those of the brake pad without groove (center). Indeed, this means that the groove plays a very important role in the thermomechanical behavior by

its design of flexibility and good resistance to wear and corrosion, thereby reducing the stress on the brake pads.

On the other hand, it can be noted that the von Mises stresses on the brake pads supported by the fixed caliper or double piston (right) are lower than those of the floating caliper (center). This means that the most favorable mode of loading which reduces the stresses is that of the double piston because it makes it possible to better distribute the braking force on the whole of the brake disc. It can be concluded that the existence of groove in the brake pad and the presence of a mechanical double piston loading have positive influence on the stress distribution on brake pad.

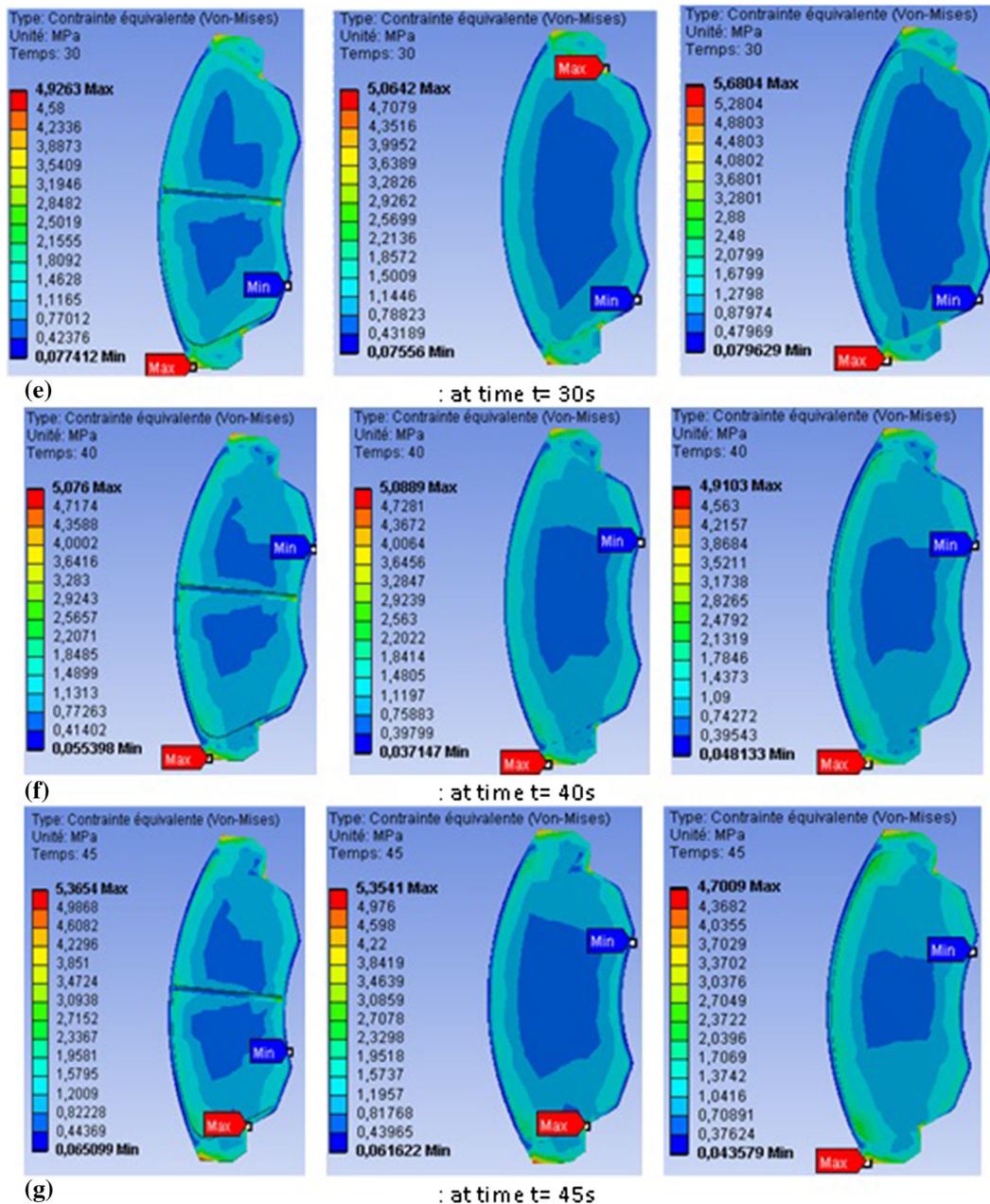


Fig. 35 continued

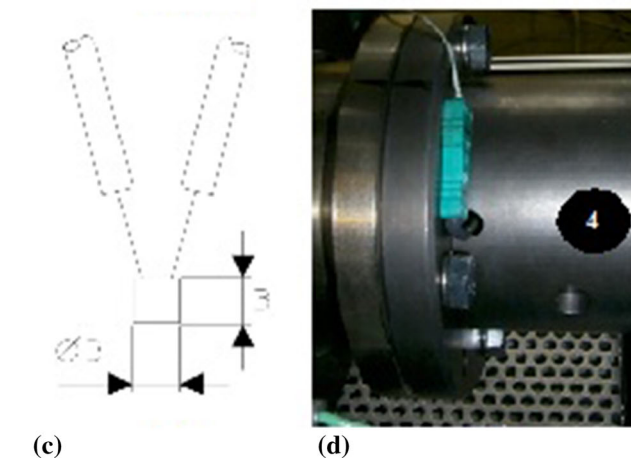
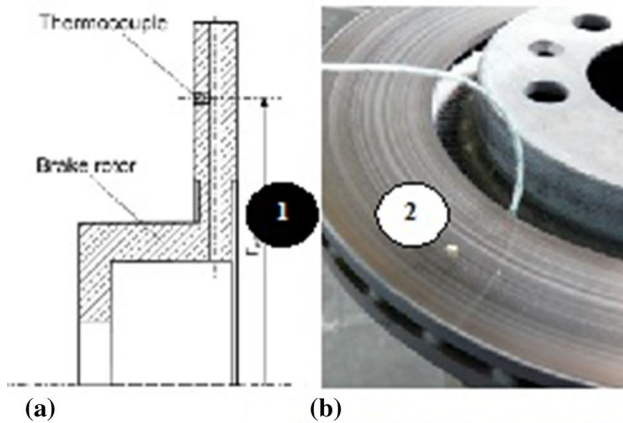


Fig. 36 Temperature measuring with embedded thermocouple as per VDA285-1

Experimental Setup

The test presented here aims to understand disc/pad interface temperature and friction in vehicle braking using an exposed thermocouple technique for interface temperature measurements and FE thermal modeling approach. The numerical results of the thermal simulation obtained in this work using ANSYS, are validated using the results of the work of Stephens [41], which was an experimental investigation on temperature distribution of ventilated disc brake rotor. The experimental study was performed to examine temperature changes on disc surfaces. In the course of the test, temperature may be measured with thermocouples installed below the friction surface of the ventilated brake disc made on gray cast of type FG15. The brake test was carried out in accordance with the assumptions of the active finite element method (FEM) which consists of looking for an approximate solution of the problem.

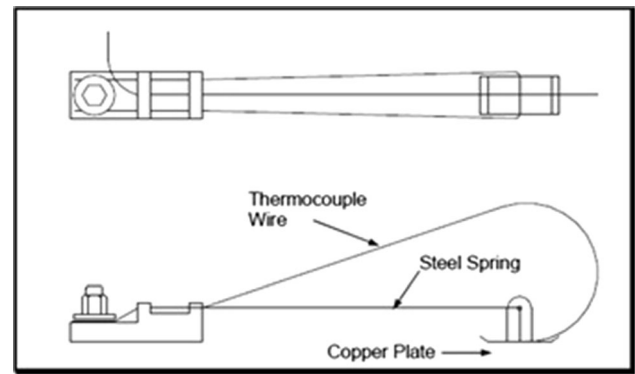


Fig. 37 Diagram of disc brake thermocouple

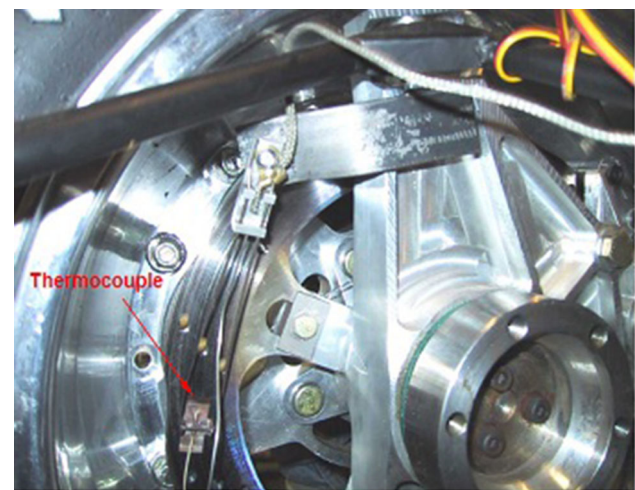


Fig. 38 Close up view of thermocouple in position

Temperature Measuring with Embedded Thermocouple

The temperature measurement was conducted using Cu thermocouples integrated in the disc brake rotors according to VDA285-1, which became accredited until the year 1996, at the mean friction radius as shown in Fig. 36a. The temperature pot-side was measured also by Cu-embedded thermocouple as shown in Fig. 36b. The thermocouples have cylindrical shape in this case with the sizes $\varnothing = 3 \text{ mm}$ and $h = 3 \text{ mm}$ as in Fig. 36c. The connecting wires were insulated on the brake rotor side and were connected to the signal amplifier.

Disc Brake Thermocouples

Thermocouples are the favored choice for testers due to their cost, ease of use and availability, and are one of the most stable methods of measuring the temperature of disc brakes in vehicles with rubbing disc brakes. The device

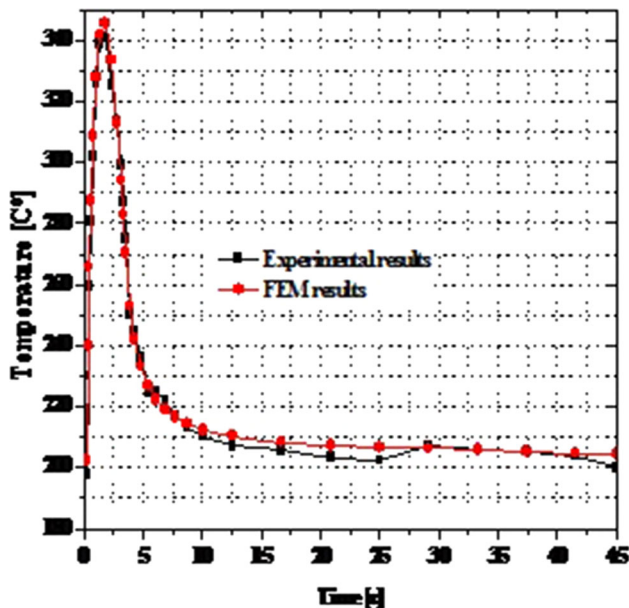


Fig. 39 Validation of the FEM model against experiments by Stephens [41]

contains K-type thermocouple, which is made using silver wire welded to a flat piece of copper plate, and this plate is strongly supported against the rotating disc by steel spring. Elementary diagram of the thermocouple is provided in Fig. 37.

Experimental Procedure

The brake was connected to the external applicator and the right rear wheel of the racing vehicle was fitted in the brake test rig as shown in Fig. 38. The rubbing thermocouple was positioned to measure the temperature on the inner surface of the rotor. The thermocouple data were recorded in the PC via a Fluke data logger.

The tests were performed by rotating the wheel at constant speed approximately equal the vehicle speed of 108 km/h. Progressive braking load was applied, and the temperatures were recorded at very short intervals of 0.01 s. The method started with the disc heating up to temperature of about 345 °C, at which point the braking load was released. The recording continued there on until the temperature of the rotor dropped to about 200 °C. The results of the thermocouple readings were obtained directly from the PC in temperature scale.

Model Validation Against Experimental Data

The analysis in this work is compared to available literature to ensure the reliability of the results. Figure 39 shows the

time variation of the observed disc temperature against the values from [41]. Figure 39 shows that the temperature results from both the thermocouple and the finite element software ANSYS 11.0 of the ventilated disc brake made of material FG15 are very similar. It is believed that the response of the thermocouple is a little slower in cooling than heating due to residual heat in its rubbing components. But the variation is small as shown in the figure, such that it was decided that the level of accuracy of rubbing type thermocouples used in the experimental stages of this research is acceptable. It can also be concluded that the transient thermal simulation of the ventilated disc, performed by the finite element method, gives us good correlation with the thermocouple measurements. The FEA approach used in this study is a very effective method for insight of the disc/pad interaction during a friction braking process.

Conclusion

In the transport sector, braking is a major problem. It is question of obtaining from this systematic safety equipment reliability with acceptable cost, whereas the phenomena which are attached to it are complex.

In general, from a thermal point of view, the braking system is considered to be composed of only three elements: the disc in motion at variable speed, on which are rubbed the two pads which are subjected to pressure evolving over time. The phenomenon of induced friction generates dissipation of thermal power at the interface and causes sharp increase in temperature that may deteriorate the equipment. The temperature level reached is directly related to the way in which the heat is transferred into its immediate environment, that is to say the disc and the two pads.

In this paper, a thermomechanical analysis of disc brake rotor with gray cast iron material properties has been performed. First, we presented complex modeling of convection-driven brake discs in order to predict the heat transfer coefficients (HTC) during the aerodynamic conditions of the braking stage by using the ANSYS CFX software.

Heat transfer coefficients (HTC) have been used in calculating the heat transfer, typically by convection or phase transition between a fluid and a solid. The heat transfer coefficients (HTC) of the brake disc's ventilation are estimated by means of a CFD computation. In this analysis, the speed of the vehicle was used to determine the heat generated by the braking taking into account all the parameters involved which affect the net heat generation and dissipation from the brake disc. Thus, we have determined the temperature rise in the brake disc and have found

a working temperature range of the brake. This technique of predicting the operating temperature of the brakes can be used for several purposes. In order to withstand both thermal and mechanical loading and knowing in advance, the operating temperature of the brakes, we can select the material used to manufacture the brake components, such as brake disc, caliper, etc.

This research was conducted to study the relationship of the brake disc geometry toward the best braking performance in term of heat dissipation in the environment. From the results, it shows that ventilated disc brake has faster heat dissipation rate to surrounding compare to full disc brake. Thus, the ventilated disc brake is having better braking performance than full disc brake in terms of heat dissipation rate. The results were also validated using the temperature–time profile from both the simulated and experimental results, in which the two results were found to be in good agreement. The literature for ventilated brake disc with gray cast iron FG15 also gives a good agreement with results from literature.

In this research, we simulated the disc-pad model by employing a coupled thermomechanical approach. From the prediction results, the following conclusions can be derived:

- At the level of outer radius and outer ring of the brake disc, large deformation occurs seriously.
- In pad without groove and that subjected to double pressure, the stresses are intensified significantly during braking.
- The temperature has significant effect on the thermo-mechanical behavior of the braking system. Thus, with thermal effect, contact pressure distribution of pad and the global deformations of the brake disc are quite important.

The temperature, stress, and total deformation of the disc and contact pressure of the pads increase due to the additional thermal stresses to the mechanical stresses, causing the fatigue cracks propagation, the fracture of the bowl, wear mechanism of the disc and brake pads. The numerical data obtained in this work are also supported by the experimental results.

However, it seems to us that several thermomechanical aspects that need to be considered in more detail in the topic of the automotive braking system, particularly for more quantitative assessment of damage in materials life approach, which are defined in perspective. Additional thermomechanical predictions could be taken into account to better interpret the effect of thermal stress migration on fatigue life of brake discs.

Conflict of interest The authors declare that there is no conflict of interest.

Appendix 1

Calculating Heat Flux Entering the Disc

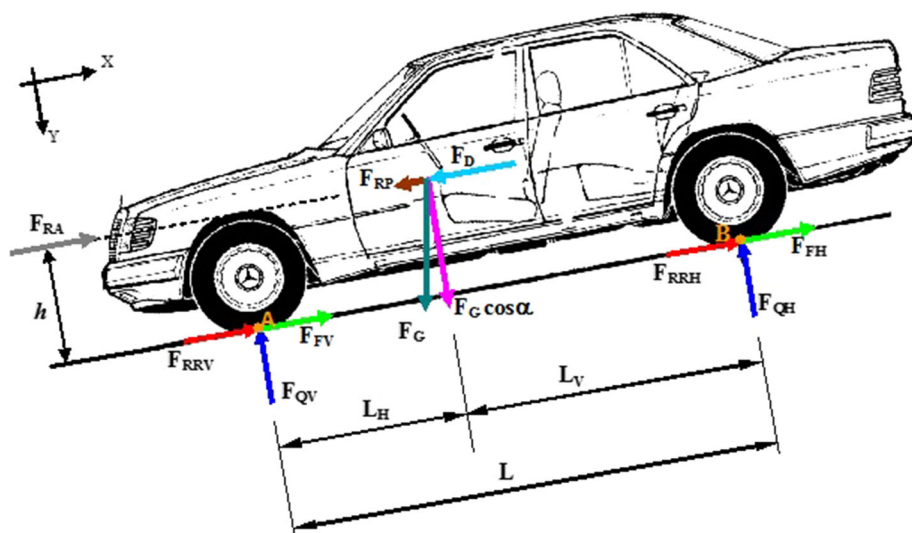
The Forces Acting on the Wheels During Braking

By observing the situation described in Fig. 40, the longitudinal and transverse equilibrium of the vehicle can be written along the local axes x, y of the car.

$$\sum F_x = 0$$

$$F_{RRV} + F_{FV} + F_{RRH} + F_{FH} + F_{RA} - (F_{RP} + F_D) = 0 \tag{Eq 28}$$

Fig. 40 Definition of the forces acting on an automobile during braking



$$F_{FV} + F_{FH} = F_{RP} + F_D - F_{RRV} - F_{RA} - F_{RRH} \quad (\text{Eq 29})$$

$$F_F = F_{RP} + F_{RF} - F_{RR} - F_{RA} \quad (\text{Eq 30})$$

with $F_F = F_{FV} + F_{FH}$, $F_{RR} = F_{RRV} + F_{RRH}$

$$\sum F_Y = 0 \Rightarrow F_G \cos \alpha - (F_{QV} + F_{QH}) = 0 \quad (\text{Eq 31})$$

$$F_{QH} = F_G \cos \alpha - F_{QV} \quad (\text{Eq 32})$$

$$\sum M_B = 0 \Rightarrow F_{QV}L + F_{RA}h - h(F_{RF} + F_{RP}) - hF_G \sin \alpha \quad (\text{Eq 33})$$

$$F_{QV} = \frac{[(F_{RF} + F_{RP})h + F_G L_H - F_{RA}h]}{L} \quad (\text{Eq 34})$$

On a road vehicle, the rolling force $F_{RR} = F_G f_r \cos \alpha$ is due to the flat formed by a tire on the road f_r is the rolling resistance coefficient. For a high pressure tire ($f_r = 0.015$).

$$F_{RP} = F_G \sin \alpha \quad (\text{Eq 35})$$

The aerodynamic force is given by:

$$F_{RA} = C_X A_F \frac{\rho_a}{2} v^2 \quad (\text{Eq 36})$$

With C_X is the coefficient of form, equal to: 0.3 to 0.4 on the car, A_F (m^2) is the frontal surface; on the approach, for a road passenger vehicle, we can take: $A_F = 0.8 \times \text{height} \times \text{width } S$ and ρ_a is the air density.

Total Braking Power

$$P_{\text{tot}} = P_R + P_F \quad (\text{Eq 37})$$

By

$$P_F = \sum F_{FV} = (F_{FV} + F_{FH})v \quad (\text{Eq 38})$$

$$P_R = \sum F_{RV} = (F_{RR} + F_{RP} + F_{RA})v \quad (\text{Eq 39})$$

In the case of flat braking (Fig. 41), the resistances due to rolling and the slope are neglected ($F_{RR} = 0$ and $F_{RP} = 0$),

the penetration into the air is generally negligible, for this reason ($F_{RA} = 0$)

$$P_R = \sum F_{RV} = (F_{RR} + F_{RP} + F_{RA})v = 0 \quad (\text{Eq 40})$$

$$P_F = \sum F_{FV} = (F_{FV} + F_{FH})v \quad (\text{Eq 41})$$

$$(F_{FV} + F_{FH}) = F_D = ma \quad (\text{Eq 42})$$

$$P_{\text{tot}} = P_F = mav \quad (\text{Eq 43})$$

If we define, Let ϕ the factor of the ratio of the braking power with respect to the rear wheels $P_{FH} = \phi mav$ then, $P_{FV} = (1 - \phi)mav$.

If a is constant, we have:

$$v(t) = v_0 - at \quad (\text{Eq 44})$$

$$P_F = (1 - \phi)ma(v_0 - at) \quad (\text{Eq 45})$$

The braking power delivered to the brake disc is equal to half the total power:

$$P_{FVI} = \frac{(1 - \phi)}{2} ma(v_0 - at) \quad (\text{Eq 46})$$

At time $t = 0$, we have

$$P_{FVI} = \frac{(1 - \phi)}{2} mav_0 \quad (\text{Eq 47})$$

The braking efficiency is then defined by the ratio between the deceleration (a) and the acceleration (g):

$$Z = a_d/g \quad (\text{Eq 48})$$

$$P_{FVI} = \frac{(1 - \phi)}{2} mZgv_0 \quad (\text{Eq 49})$$

Assuming that the amount of heat generated by friction is completely absorbed by the disc.

Fig. 41 External forces acting on the vehicle during braking on a flat road

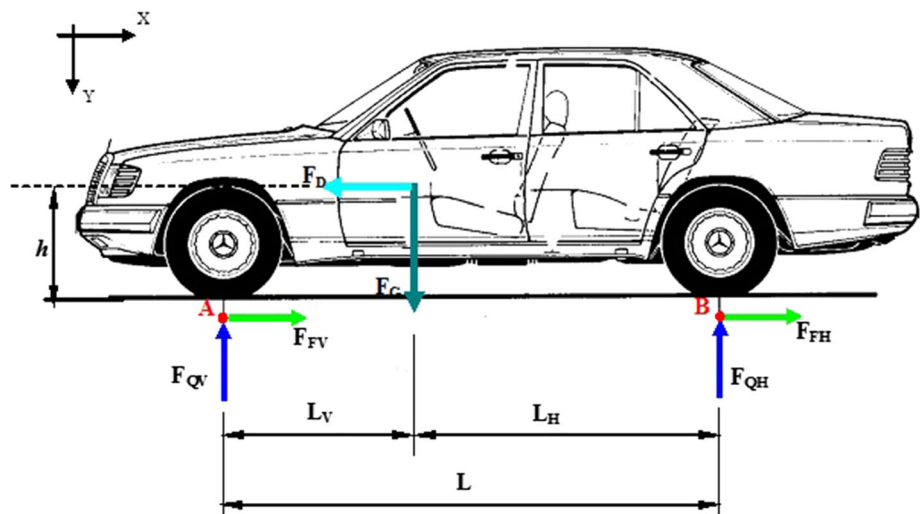
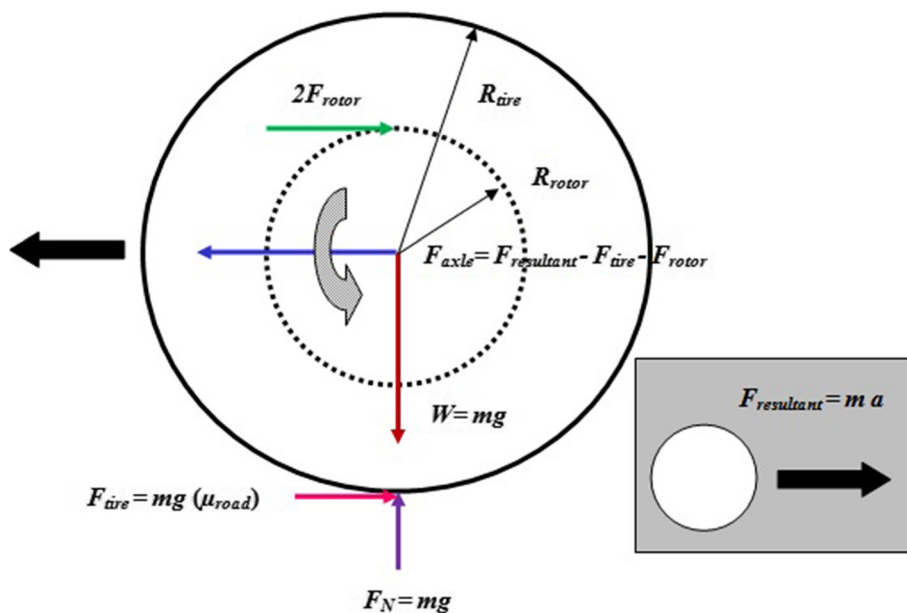


Fig. 42 Free body diagram of a front wheel-rotor system



$$Q_v = \frac{(1 - \phi)}{2} m_{tot} g v \quad [\text{Nm/s}] = [\text{W}] \quad (\text{Eq 50})$$

The expression of the transformed friction power per unit area is thus:

$$Q'_v = \frac{(1 - \phi) m_{tot} g v}{2 A_d} \quad [\text{N m/s m}^2] = [\text{W/m}^2] \quad (\text{Eq 51})$$

The quantity Q'_v indicates the heat flow absorbed by the disc, which must be housed only on the actual contact surface. Where A_d is the surface of the rotor to which a brake pad pivots.

By definition, the operating factor ϵ_p of the friction surface is given by the following formula:

$$\epsilon_p = Q'_v / Q'_{v_{max}} \quad (\text{Eq 52})$$

Thus, the equation of the initial thermal flow of friction entering the disc, which is calculated as follows:

$$Q'_{v_{max}} = \frac{(1 - \phi) m_{tot} g v}{2 A_d} \quad [\text{N m/s m}^2] = [\text{W/m}^2] \quad (\text{Eq 53})$$

Appendix 2

Analysis of Disc Rotor Force

A free body diagram of a front wheel-rotor system, Fig. 42, is used to drive the equation of equilibrium. Since large amount of the braking load is born by the front brakes, that amount of kinetic energy and potential energy into a single disc is given by

$$E_{dissipated} = \frac{1}{2} k m v_0^2 + S_b m g \sin \alpha \quad (\text{Eq 54})$$

But $S_b = \frac{v_a^2}{2a}$

$$E_{dissipated} = \frac{1}{2} k m v_0^2 + \frac{v_0^2}{2a} m g \sin \alpha \quad (\text{Eq 55})$$

The power dissipated by each rotor face is equal to the heat flux into the rotor face.

$$E_{dissipated} = \int P_{dissipated} t dt = \int (2F_{rotor}) v_{rotor}(t) dt \quad (\text{Eq 56})$$

$$\begin{aligned} \frac{1}{2} k m v_0^2 + \frac{v_0^2}{2a} m g \sin \alpha &= KE_{dissipated} = \int P_{dissipated} t dt \\ &= 2 \int F_{rotor} v_{rotor}(t) dt \end{aligned} \quad (\text{Eq 57})$$

But from kinematic relationships.

$$\begin{aligned} v_{vehicle}(t) &= v_0 - at \\ a &= \frac{v_0}{t_{stop}} \\ \frac{v_{vehicle}(t)}{R_{tire}} &= \omega(t) = \frac{v_{rotor}(t)}{R_{rotor}} \\ v_{rotor}(t) &= \frac{R_{rotor}}{R_{tire}} \left(v_0 - \left\{ \frac{v_0}{t_{stop}} \right\} t \right) \end{aligned}$$

F_{rotor} is constant with respect to time, and v_{rotor} varies only linearly with time so the energy balance equation becomes:

$$\frac{1}{2}kmv_0^2 + \frac{v_0^2}{2a}mg \sin \alpha = 2F_{\text{rotor}} \int_0^{t_{\text{stop}}} v_{\text{rotor}}(t) dt \quad (\text{Eq 58})$$

$$= 2F_{\text{rotor}} \frac{R_{\text{rotor}}}{R_{\text{tire}}} \left(v_0 t_{\text{stop}} - \frac{1}{2} \left\{ \frac{v_0}{t_{\text{stop}}} \right\} t_{\text{stop}}^2 \right)$$

$$F_{\text{rotor}} = \frac{\frac{1}{2}kmv_0^2 + \frac{v_0^2}{2a}mg \sin \alpha}{2 \frac{R_{\text{rotor}}}{R_{\text{tire}}} \left(v_0 t_{\text{stop}} - \frac{1}{2} \left\{ \frac{v_0}{t_{\text{stop}}} \right\} t_{\text{stop}}^2 \right)} \quad (\text{Eq 59})$$

When braking on a straight/flat track ($\alpha = 0$), k is estimated to be about 0.30. Therefore, Eq 59 should be modified to be:

$$F_{\text{disc}} = \frac{(30\%) \frac{1}{2}mv_0^2}{2 \frac{R_{\text{rotor}}}{R_{\text{tire}}} \left(v_0 t_{\text{stop}} - \frac{1}{2} \left\{ \frac{v_0}{t_{\text{stop}}} \right\} t_{\text{stop}}^2 \right)} \quad (\text{Eq 60})$$

References

- R. Leal, F.M. Barreiros, L. Alves, F. Romeiro, J.C. Vasco, M. Santos, C. Marto, Additive manufacturing tooling for the automotive industry. *Int. J. Adv. Manuf. Technol.* **92**, 1671–1676 (2017)
- W.H. Li, H. Du, Design and experimental evaluation of a magneto rheological brake. *Int. J. Adv. Manuf. Technol.* **21**, 508–515 (2003)
- R. Udayakumar, R. Ponnusamy, Computer aided design and analysis of disc brake rotors for passenger cars, in *International Conference on Computer Applications Technology, ICCAT 2013* (2013), pp. 1–5. <https://doi.org/10.1109/iccat.2013.6521979>
- P. Sadagopan, H.K. Natarajan, P. Kumar, Study of silicon carbide-reinforced aluminum matrix composite brake rotor for motorcycle application. *Int. J. Adv. Manuf. Technol.* **94**, 1461–1475 (2018)
- Pei-Lum Tso, Rick Hsu, Estimating chemical mechanical polishing pad wear with compressibility. *Int. J. Adv. Manuf. Technol.* **32**, 682–689 (2007)
- N.Y. Nguyen, Z.W. Zhong, Y.B. Tian, Analysis and improvement of the pad wear profile in fixed abrasive polishing. *Int. J. Adv. Manuf. Technol.* **85**, 1159–1165 (2016)
- C.-C.A. Chen, Q.-P. Pham, Study on diamond dressing for non-uniformity of pad surface topography in CMP process. *Int. J. Adv. Manuf. Technol.* **91**, 3573–3582 (2017)
- S. Hasagasioglu, K. Kilicaslan, O. Atabay, A. Güney, Vehicle dynamics analysis of a heavy-duty commercial vehicle by using multibody simulation methods. *Int. J. Adv. Manuf. Technol.* **60**, 825–839 (2012)
- M.A. Ashraf, B. Sobhi-Najafabadi, Ö. Göl, D. Sugumar, Numerical simulation of sliding wear for a polymer–polymer sliding contact in an automotive application. *Int. J. Adv. Manuf. Technol.* **41**, 1118–1129 (2009)
- K. Salonitis, P. Stavropoulos, A. Kolios, External grind-hardening forces modelling and experimentation. *Int. J. Adv. Manuf. Technol.* **70**(1–4), 523–530 (2014)
- P.M. Lerones, J.L. Fernández, J.G. García-Bermejo, E. Zalama, Total quality control for automotive raw foundry brake disks. *Int. J. Adv. Manuf. Technol.* **27**, 359–371 (2005)
- Y.A. Çengel, A.J. Ghajar, *Heat and Mass Transfer: Fundamentals & Applications* (McGraw-Hill, New York, 2011)
- A. Belhocine, N.M. Ghazaly, Effects of young's modulus on disc brake squeal using finite element analysis. *Int. J. Acoust. Vib.* **31**(3), 292300 (2016)
- M.R. Ishak, A.R. Abu Bakar, A. Belhocine, J.M. Taib, W.Z. Wan Omar, Brake torque analysis of fully mechanical parking brake system: Theoretical and experimental approach. *Ing. Investig. Technol.* **19**(1), 37–49 (2018)
- J.H. Choi, I. Lee, Transient thermoelastic analysis of disk brakes in frictional contact. *J. Therm. Stress.* **26**(3), 223–244 (2003)
- J.H. Choi, I. Lee, Finite element analysis of transient thermoelastic behaviors in disk brakes. *Wear* **257**(1–2), 47–58 (2004)
- Y. Yildiz, M. Duzgun, Stress analysis of ventilated brake discs using the finite element method. *Int. J. Automot. Technol.* **11**(1), 133–138 (2010)
- Adam Adamowicz, Piotr Grzes, Influence of convective cooling on a disc brake temperature distribution during repetitive braking. *Appl. Therm. Eng.* **31**(14–15), 2177–2185 (2011)
- M. Duzgun, Investigation of thermo-structural behaviors of different ventilation applications on brake discs. *J. Mech. Sci. Technol.* **26**(1), 235–240 (2012)
- M. Pevec, Prediction of the cooling factors of a vehicle brake disc and its influence on the results of a thermal numerical simulation. *Int. J. Automot. Technol.* **13**(5), 725–733 (2012)
- P. Hwang, X. Wu, Investigation of temperature and thermal stress in ventilated disc brake based on 3d thermo-mechanical coupling model. *J. Mech. Sci. Technol.* **24**(1), 81–84 (2010)
- M.J. Han, C.H. Lee, T.W. Park, S.P. Lee, Low and high cycle fatigue of automotive brake discs using coupled thermo-mechanical finite element analysis under thermal loading. *J. Mech. Sci. Technol.* **32**(12), 5777–5784 (2018)
- M.J. Han, C.H. Lee, T.W. Park, J.M. Park, S.M. Son, Coupled thermo-mechanical analysis and shape optimization for reducing uneven wear of brake pads. *Int. J. Automot. Technol.* **18**(6), 1027–1035 (2017)
- P. Dufrénoy, D. Weichert, Prediction of railway disc brake temperatures taking the bearing surface variations into account. *Proc. Inst. Mech. Eng. Part F J. Rail Rapid Transit* **209**(2), 67–76 (1995)
- E. Palmer, R. Mishra, J.D. Fieldhouse, An optimization study of a multiple row pin vented brake disc to promote brake cooling using computational fluid dynamics. *Proc. Inst. Mech. Eng. Part D J. Automob. Eng.* **223**(7), 865–875 (2009)
- J. Reimpel, *Braking Technology* (Vogel Verlag, Würzburg, 1998)
- C. Cruceanu, *Frâne pentru vehicule feroviare (Brakes for railway vehicles)*, Ed. MATRIXROM, București (2007). ISBN: 978-973-755-200-6
- H. Dittrich, R. Lang, Finite-Element Analysis of the thermal loads acting on a passenger car brake disk. *Automob. Z.* **86**(6), 265–269 (1984)
- A. Fukano, H. Matsui, Development of disc-brake design method using computer simulation of heat phenomena, SAE 860634 (1986)
- P.F. Gotowicki, V. Nigrelli, G.V. Mariotti, D. Aleksendric, C. Duboka, Numerical and experimental analysis of a pegs-wing ventilated disk brake rotor with pads and cylinders, in *10th EAEC European Automotive Congress—Paper EAEC05YUAS04–P5* (2005)
- K. Rajesh, Transient thermoelastic analysis of disk brake using ANSYS software, M.Tech thesis, Thapar University, 2008
- R. Limpert, *Brake Design and Safety*, 3rd edn. (SAE International, Warrendale, 2011), pp. 1–112
- M.K. Khalid, M.R. Mansor, S.I. Abdul Kudus, M.M. Tahir, M.Z. Hassan, Performance investigation of the UTEM eco-car disc brake. *Syst. Int. J. Eng. Technol.* **11**(6), 1–6 (2011)
- R. Limpert, *Brake Design and Safety*, 2nd edn. (Society of Automotive Engineering Inc., Warrendale, 1999), pp. 137–144

35. M. Burckhardt, *Fahrwerktechnik: Bremsdynamik und PKW-Bremsanlagen* (Vogel Buchverlag, Würzburg, 1991)
36. J. Zhang, C. Xia, Research of the transient temperature field and friction properties on disc brakes, in *Proceedings of the 2012 2nd International Conference on Computer and Information Application (ICCIA 2012)* (2012), pp. 201–204
37. T.J. Mackin, S.C. Noe, K.J. Ball, B.C. Bedell, D.P. Bim-Merle, M.C. Bingaman, D.M. Bomleny, G.J. Chemlir, D.B. Clayton, H.A. Evans, Thermal cracking in disc brakes. *Eng. Fail. Anal.* **9**, 63–76 (2002)
38. G. Oder, M. Reibenschuh, T. Lerher, M. Šraml, B. Šamec, I. Potrč, Thermal and stress analysis of brake discs in railway vehicles. *Adv. Eng.* **3**(1), 95–102 (2009)
39. N. Coudeyras, Non-linear analysis of multiple instabilities to the rubbing interfaces: application to the squealing of brake, PhD Thesis, Central school of Lyon-speciality: mechanics, 2009
40. A.R. Abu Bakar, H. Ouyang, L.C. Khai, M.S. Abdullah, Thermal analysis of a disc brake model considering a real brake pad surface and wear. *Int. J. Veh. Struct. Syst.* **2**(1), 20–27 (2010)
41. Stephens, A. Aerodynamic cooling of automotive disc brakes, Master's thesis, School of Aerospace, Mechanical and Manufacturing Engineering, RMIT University, 2006

Publisher's Note Springer Nature remains neutral with regard to jurisdictional claims in published maps and institutional affiliations.